



Assistive Exoskeleton for Injury Prevention During Downhill Walking

Citation

Rogers, Emily Ann. 2015. Assistive Exoskeleton for Injury Prevention During Downhill Walking. Bachelor's thesis, Harvard College.

Permanent link

<http://nrs.harvard.edu/urn-3:HUL.InstRepos:14398554>

Terms of Use

This article was downloaded from Harvard University's DASH repository, and is made available under the terms and conditions applicable to Other Posted Material, as set forth at <http://nrs.harvard.edu/urn-3:HUL.InstRepos:dash.current.terms-of-use#LAA>

Share Your Story

The Harvard community has made this article openly available.
Please share how this access benefits you. [Submit a story](#).

[Accessibility](#)

Assistive Exoskeleton for Injury Prevention During Downhill Walking

by
Emily Ann Rogers

ES 100 Project Report submitted to the School of Engineering and Applied Sciences in partial fulfillment of the requirements for the degree of

Bachelor of Science (S.B.) in Engineering Sciences with specialization in Bioengineering

at

Harvard University
Spring 2015

Submitted by
School of Engineering and Applied Sciences
April 2, 2015

Supervised and Evaluated by
Dónal Holland
Visiting Lecturer in Engineering Sciences

Supervised and Evaluated by
Panagiotis Polygerinos
Technology Development Fellow, Wyss Institute

Evaluated by
Conor J. Walsh
Assistant Professor of Mechanical and Biomedical Engineering

Abstract

This thesis presents a device designed to reduce muscular effort during downhill walking. The designed solution is a soft wearable exoskeleton consisting of an air spring, a wearable soft fabric interface that attaches the air spring to the user's body, and an integrated smart sensing and pneumatic control system. After prototyping of the device, initial evaluation was performed, showing that the device successfully produced a resistive torque of 5 Nm, decreasing torque on the knee by 10% for a 58 kg individual on a -20 degree slope. Following initial evaluation, human subject testing was conducted in order to determine the effect of the device on muscle activity and gait. Initial results show that on a -5 degree slope, the device can reduce muscle activity by up to 17%. Additionally, joint angle data showed that there were no substantial negative effects on the users natural gait pattern. This device is a low-cost solution that will help the active, elderly, and physically impaired alike by decreasing muscle fatigue, decreasing risk of overuse injuries, increasing independence, and improving overall quality of life.

Thesis Supervisor: Dónal Holland

Title: Visiting Lecturer in Engineering Sciences

Thesis Supervisor: Panagiotis Polygerinos

Title: Technology Development Fellow, Wyss Institute

Contents

Preface	i
Abstract	i
List of Figures	vi
List of Tables	xi
1 Introduction	1
1.1 Motivation	1
1.2 Prior Art	2
1.2.1 Passive Devices	2
1.2.2 Active Devices	3
1.2.3 Area of Opportunity	4
1.3 Thesis Overview	5
2 Background Research	9
2.1 User Needs	9
2.2 Biomechanics	10
2.3 Functional Requirements	14
3 Design	17
3.1 Design Development	17
3.1.1 Concept 1: Leaf Spring	17
3.1.2 Concept 2: Torsional Spring	19
3.1.3 Concept 3: Air Spring	20

3.1.4	Design Selection	22
3.2	Final Design	24
3.2.1	Air Spring	24
3.2.2	Interface	26
3.2.3	Sensing and Control	27
3.3	Design Evolution	29
3.4	Design Evaluation	30
3.4.1	Device Mass	30
3.4.2	Power Requirements	30
3.4.3	Characterization of Air Spring	31
4	Testing and Results	35
4.1	Human Subject Testing	35
4.2	Analysis	37
4.3	Results	37
5	Conclusion	41
5.1	Conclusion	41
5.2	Future Work	42
Acknowledgements		43
A Additional Testing Results		45
A.1	Additional EMG Data Plotted by Slope	45
A.2	Muscle Activity and Standard Deviation	50
A.3	Ground Reaction Force	56
A.4	Joint Angles	58
B Bill of Materials		59
C Engineering Drawings		63
D Code		69

E Survey Data **73**

References **76**

List of Figures

1-1	Passive devices	2
1-2	Active devices	3
1-3	Previous design of assistive exoskeleton for downhill walking	4
1-4	System overview	5
2-1	Interest in assistive device	9
2-2	Knee pain experienced while hiking	10
2-3	Gait cycle	10
2-4	Knee kinematics	11
2-5	Free body diagram	12
2-6	Knee moment during downhill walking	13
2-7	Knee angle during downhill walking	13
2-8	Peak torque during downhill walking	15
2-9	Metabolic rate vs. load	16
3-1	Concept development	17
3-2	Leaf spring design implemented in hopping device	18
3-3	Leaf spring calculations	18
3-4	Torsional spring diagram	19
3-5	Air spring diagram	20
3-6	Air spring theoretical force profile	21
3-7	Air spring attachment point, force requirement, and radius	22
3-8	Final design overview	23
3-9	Air spring final design	24

3-10 Air spring valves	25
3-11 Interface overview	26
3-12 Device control flow chart	27
3-13 Foot switches	27
3-14 Electronic control circuit	28
3-15 Control valve	29
3-16 Design evolution of interface	29
3-17 Air spring characterization under unilateral compression	31
3-18 Force profile of air spring	32
3-19 Torque vs. air spring radii and length	33
3-20 Torque generated by air spring on varying slopes	33
4-1 Human subject testing	35
4-2 Electrode placement	37
4-3 Vastus medialis average muscle activity	38
4-4 Rectus femoris average muscle activity	38
4-5 Vastus medialis total integrated muscle activity	39
4-6 Rectus Femoris total integrated muscle activity	39
4-7 Joint angle during device testing	40
A-1 Vastus medialis 0 degrees	45
A-2 Rectus femoris 0 degrees	46
A-3 Biceps femoris 0 degrees	46
A-4 Vastus medialis -5 degrees	47
A-5 Rectus femoris -5 degrees	47
A-6 Biceps femoris -5 degrees	48
A-7 Vastus medialis -15 degrees	48
A-8 Rectus femoris -15 degrees	49
A-9 Biceps femoris -15 degrees	49
A-10 Vastus medialis -5 degrees active	50
A-11 Vastus medialis -5 degrees inactive	50

A-12 Vastus medialis -5 degrees control	51
A-13 Vastus medialis -15 degrees active	51
A-14 Vastus medialis -15 degrees inactive	51
A-15 Vastus medialis -15 degrees control	52
A-16 Rectus femoris -5 degrees active	52
A-17 Rectus femoris -5 degrees inactive	52
A-18 Rectus femoris -5 degrees control	53
A-19 Rectus femoris -15 degrees active	53
A-20 Rectus femoris -15 degrees inactive	53
A-21 Rectus femoris -15 degrees control	54
A-22 Biceps femoris -5 degrees active	54
A-23 Biceps femoris -5 degrees inactive	54
A-24 Biceps femoris -5 degrees control	55
A-25 Biceps femoris -15 degrees active	55
A-26 Biceps femoris -15 degrees inactive	55
A-27 Biceps femoris -15 degrees control	56
A-28 Ground reaction force: 0 Degrees	56
A-29 Ground reaction force: -5 degrees	57
A-30 Ground reaction force: -15 degrees	57
A-31 Joint angle: -15 degrees	58
C-1 Engineering drawing: top air spring end cap	64
C-2 Engineering drawing: bottom air spring end cap	65
C-3 Engineering drawing: rod attachment piece	66
C-4 Cylinder piston datasheet showing part dimensions	67

List of Tables

2.1	Functional Requirements	14
3.1	Pugh matrix	23
3.2	Mass of device components	30
4.1	Testing protocol	36
4.2	Trials measured during testing	36
B.1	Total Cost of Prototyping	60
B.2	Cost of Final Prototype	61

Chapter 1

Introduction

1.1 Motivation

Downhill walking is an integral part of our daily lives. From navigating the stairs in the home and workplace, to performing recreational activities such as hiking, our ability to walk downhill safely and comfortably is important for our productivity, health, and well-being. Forces on the knee are much greater during downhill walking than on level surfaces. The knee acts as a torque damping mechanism, a brake that counteracts the force of gravity to slow the bodies descent. This additional stress can lead to fatigue, muscle injury, and degenerative joint diseases. From elderly people navigating the stairs in their home, to active hikers that frequently descend mountainous terrain, knee injuries prevent many individuals from performing activities that are necessary for an independent and enjoyable life.

This thesis presents the design, fabrication, and testing of a lightweight wearable device that reduces the muscular effort and physical stress on the knee during downhill walking. This device is a wearable exoskeleton consisting of an air spring that provides a resistive torque at the knee, a wearable fabric interface for secure and comfortable device attachment, and an integrated sensing and pneumatic control system that adapts to the users natural gait and walking pace. By augmenting healthy individuals and assisting impaired individuals, this device has the ability to improve quality of life, prevent injuries, and increase independence for potential users.



(a) Hiking Poles [1]



(b) Supportive Knee Brace [2]

Figure 1-1: Passive devices currently available for additional support during downhill walking.

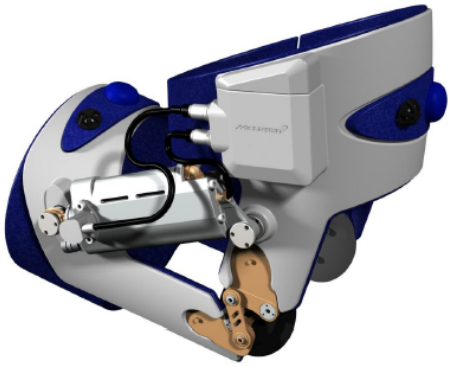
1.2 Prior Art

There have been many attempts to develop devices to augment human ability and assist activities of daily living. Previously designed devices for downhill walking assistance fall into two main categories: passive devices (figure 1-1), which provide additional support to the wearer in an attempt to stabilize joints, and active devices (figure 1-2), which require an energy input in order to generate an assistive force.

1.2.1 Passive Devices

Passive assistive devices such as knee braces and hiking poles are widely available and relatively inexpensive. However, because they reinforce the knee, rather than providing additional assistive forces, their benefits are limited. Hiking poles (figure 1-1a) have been demonstrated to reduce exercise induced muscle damage and muscle soreness during and after hiking descents [3]. However, poles reduce stress on the knees by redistributing the forces to other areas of the user's body, specifically the arms [3]. Drawbacks of the use of hiking poles include increased muscle soreness of the upper body, and decreased agility and coordination - because the user's hands must hold the poles.

Off the shelf knee braces (figure 1-1b) have been shown to effectively provide increased protection to the knee. In contact sports, they have been shown to reduce



(a) Bionex [5]



(b) Bionic Power [6]

Figure 1-2: Active devices designed to reduce torque on the users knee during walking.

medial collateral ligament injuries by 20-30% [4]. However, knee braces have a minimal effect on reducing torque about the knee, the main source of increased force and stress during downhill walking.

1.2.2 Active Devices

The Bionex knee brace (figure 1-2a), designed by the Bio-Mechatronics division of JRi Shocks, is a carbon fiber brace that damps knee flexion to reduce impact on the joint [5]. This device consists of a 4-bar linkage hinge joint to replicate the biological motion of the knee, and a neoprene and nylon fastening system, with an inflatable bladder that expands and shrinks to accommodate knee swelling [5]. This device uses a wireless Bluetooth sensing system during its ‘intuitive’ control mode which allows the brace to automatically lock into safety mode if motion outside of a preset range is detected. The maximum allowable joint angle and speed is set by the user, and the use of Magna Rheological fluids allows the resistance of the damper to be controlled precisely. This device weighs 0.70 kg per leg [5].

A biomechanical energy harvester device designed by Bionic Power (figure 1-2b), applies a resistive torque to the knee joint during walking and translates this mechanical energy into electricity [6]. This device weighs only 1.7 kg and consists of an aluminum chassis and generator mounted on a knee brace [6]. It is capable of producing 6.4 Nm of resistive torque while simultaneously converting 54% of this power

into electricity, producing from 5-16.8 V and 8-14 W [6]. While this device effectively harnesses electrical energy from mechanical energy, it provides minimal assistance during walking.

While active devices are generally capable of providing a greater amount of assistance than passive devices, their complexity, cost, and power requirements make them inaccessible to most of the people who would benefit from them.

1.2.3 Area of Opportunity

This thesis aims to fill the current gap between active and passive technologies. By designing a semi-active device, this project attempts to create a device that provides a greater amount of assistance than completely passive devices, while remaining more affordable, light weight, and accessible than current active technologies.



Figure 1-3: Previous design of an exoskeleton to assist downhill walking [7].

A previous attempt to fill this gap was presented in the thesis Exoskeleton to Assist Downhill Walking, as an Engineering Sciences 100 project in 2014 [7]. This device consists of a carbon fiber knee exoskeleton with integrated sensors and a clutching mechanism to engage and disengage the resistive mechanism during appropriate phases of the gait. This device is able to apply a 17 Nm peak resistive torque at the knee, approximately 25% of the torque on the knee of a 80 kg person during walking on a slope of -9 degrees. Using a preliminary sensing mechanism, the device is able to approximately sense the stance phase of the gait cycle. If the current one-legged

prototype were to be extended to both legs, the device would weigh 4.4 kg.

This thesis aims to improve upon the previous device by developing a lighter weight, soft wearable device, that is capable of providing a comparable resistive torque at the knee. This iteration is designed and prototyped for a two-leg device, and more extensive testing and analysis was performed.

1.3 Thesis Overview

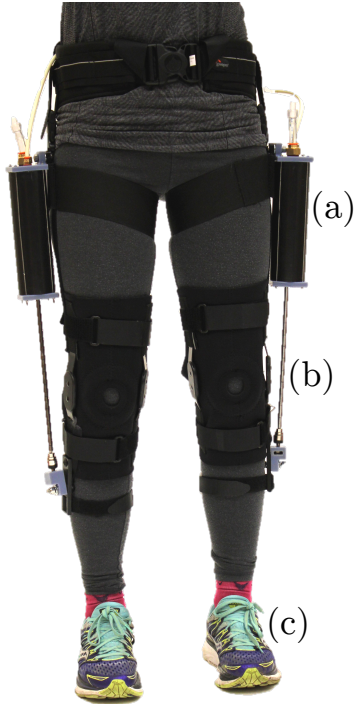


Figure 1-4: System overview: (a) air spring, (b) interface, (c) sensing and control.

The system shown in figure 1-4 was developed to decrease the amount of torque applied to the user's knees during downhill walking. The device is lightweight, comfortable, and provides assistance during the stance phase of the gait cycle while providing minimal resistance during the swing phase. User needs research was conducted in order to identify the area of opportunity, and biomechanics research identified the portion of the gait cycle during which forces on the knee are the greatest. From these initial findings, functional requirements for the device were determined in order to define design concepts. From the initial designs, an air spring design was chosen for

the final prototype. This design consists of an air spring that generates a resistive torque about the user's knee, a comfortable device/human interface, and a smart sensing and control system (figure 1-4).

Following the design of the device, evaluation and human subject testing was conducted in order to quantify device performance. Initial human subject testing showed a decrease in muscle activity of up to 17% while walking on a -5 degree slope.

Through the design of a wearable exoskeleton, it was shown that the load on the wearer's knees during downhill walking can be reduced. The device successfully met the functional requirements of providing a resistive torque at the knee, reducing total torque by 10% for a 58 kg individual on a -20 degree slope. This device incorporates a smart sensing and control system by activating the exoskeleton to reduce torque during the stance phase of walking, and disengaging during the swing phase to avoid inhibition of the natural gait.

Knee injuries have a high societal cost due to lost wages, productivity, and disability. Knee osteoarthritis alone, a condition characterized by cartilage and bone damage linked to overuse and excessive joint stress, affects 33.6% of adults ages 65+ [8]. In todays aging population the prevalence continues to rise, and creating a device to help prevent and alleviate knee injuries could improve the lives of many. By decreasing the prevalence and severity of injuries, this device will also help decrease the high medical costs, which amount to \$5,700 per patient per year for osteoarthritis alone [8]. Additionally, decreasing the rate of disability due to knee injuries will decrease the high earning losses of \$13.2 billion per year [8].

By researching an often overlooked area of human gait assistance, this thesis will benefit and promote future research targeting downhill walking assistive devices. This technology also has the potential to be translated to a load carrying device to assist with the carrying of heavy loads for long distances. This thesis presents a fully wearable, portable, lightweight device. It has been shown to provide an up to 17% decrease in muscle activity, helping decrease muscle fatigue, allowing the wearer to be active longer without over-stressing their knees. This device has the potential to increase the physical ability and independence of a range of individuals. This is a

low-cost solution that will help the active, elderly, and physically impaired alike by decreasing muscle fatigue, decreasing risk of overuse injuries, increasing independence, and improving overall quality of life.

Chapter 2

Background Research

2.1 User Needs

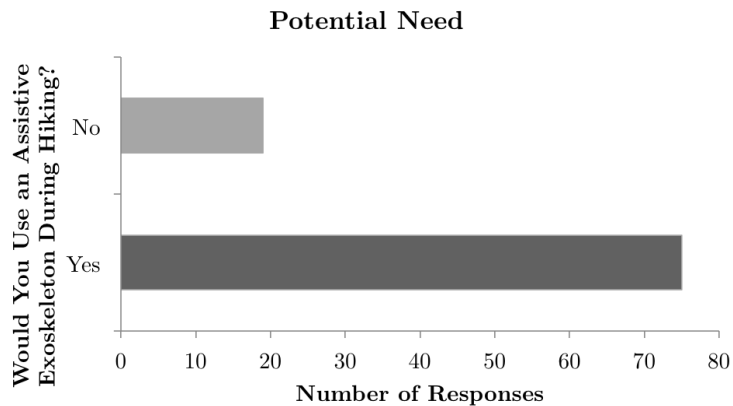


Figure 2-1: Potential users were surveyed to determine need for an assistive exoskeleton. Across all age groups, the majority of respondents indicated that they would use an assistive exoskeleton while hiking ($n=94$).

In order to evaluate need for an assistive device, individuals of the target population were surveyed as part of the background research for this project. Responses from 94 active individuals of ages 18-60+ were collected (complete list of survey responses in appendix E). Of the respondents, 16% had previously injured their knee while hiking. 45% currently use an assistive device such as hiking poles or knee braces while hiking. Over 75% of respondents indicated that they would wear an assistive exoskeleton during hiking - showing that there is high demand for additional assistance

during downhill walking (figure 2-1). Additionally, 68% of respondents experience knee pain during or after downhill walking (figure 2-2).

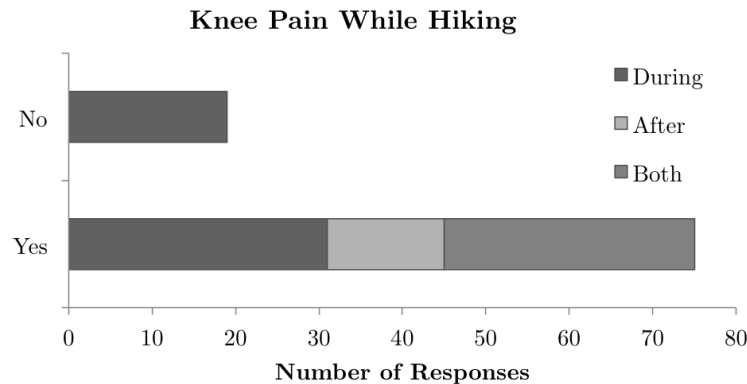


Figure 2-2: More than 75% of surveyed individuals had experienced knee pain either during or after hiking (n=94).

2.2 Biomechanics

An extensive literary review and biomechanics testing were performed in order to gain a thorough understanding of the biomechanics of human walking. Figure 2-3 shows images of the phases of walking throughout the gait cycle.

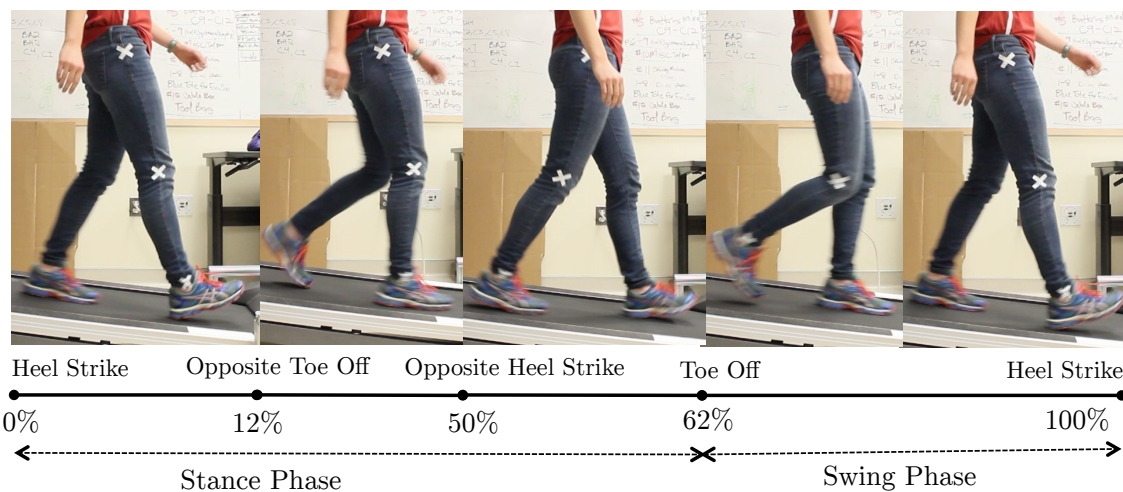


Figure 2-3: Gait cycle on -8.5 degree slope: stance phase, when the foot is in contact with the ground (0-62%), and swing phase, when foot is lifted off the ground (62-100%).

The main phases of the gait cycle are stance, which occurs from heel strike until toe off (0-62%), and swing, which occurs from toe off until opposite heel strike (62-100%). Video analysis software was used to study the downhill walking gait on a -8.5 degree slope [9]. Using the measured joint angles from video analysis, a free body diagram (figure 2-5) was created to estimate the torque on the knee during the stance phase of walking. Because the proposed device will assist walking by reducing torque on the knee during stance, torque analysis was limited to the stance phase of walking.

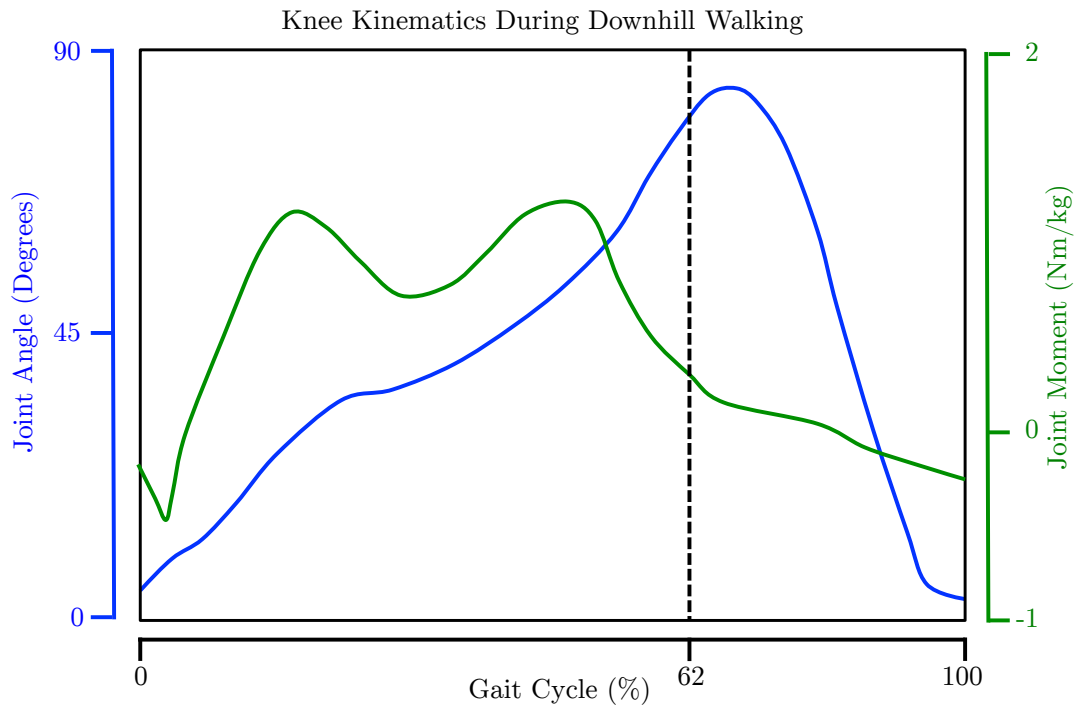


Figure 2-4: Kinematic knee data for walking on a -21 degree slope (adapted from [10] and [11]) Knee angle in blue (the neutral stance position represents 0 degrees) and joint moment in green (positive moments indicate extensor) normalized to body mass.

The main differences between downhill walking and level walking are that during downhill walking, the knee undergoes greater flexion during the stance phase in order to lower the body down the slope [10]. Additionally, on downhill slopes the knee moment remains extensor during mid and late stance as they brake the bodies

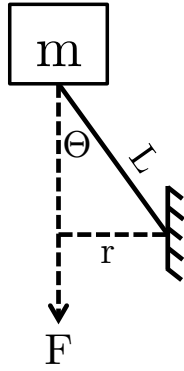


Figure 2-5: Free body diagram, L is the length of the thigh, m represents the body mass, assumed to be located entirely at the center of mass, and the knee is represented as a fixed point which the leg may rotate about. Theta represents hip angle.

acceleration due to gravity, while these portions of the gait cycle are flexor during level walking [10]. Joint angle and torque are shown for the entire gait cycle (figure 2-4). Figure 2-4 shows two peaks in moment, signifying weight transfer and push-off. While the magnitude of the moments are equivalent for the two peaks, the second peak occurs when the knee is at a higher degree of flexion and when a larger amount of power is being dissipated by the knee extensor muscles.

$$\tau = F \times r = m \times g \times l \times \sin \theta \quad (2.1)$$

Where: F = Force,

r = Radius,

τ = Torque,

m = Body mass,

g = Acceleration due to gravity,

l = Length of thigh,

θ = Hip angle

For this reason, risk of muscle fatigue and knee injuries are higher during this second peak in moment. Therefore, when determining the requirements for an assis-

tive device the maximum amount of assistance should be applied during the second peak in joint torque, at approximately 50% of the gait cycle. An ideal device would therefore provide the greatest amount of assistance at 50% of the gait cycle.

Using a simplified model of the forces on the knee during walking (figure 2-5), torque is calculated in equation 2.1. Because the acceleration due to angular velocity at the knee is negligible during stance phase compared to that during swing phase, it is assumed that acceleration due to gravity is the only non-negligible force on the body during stance.

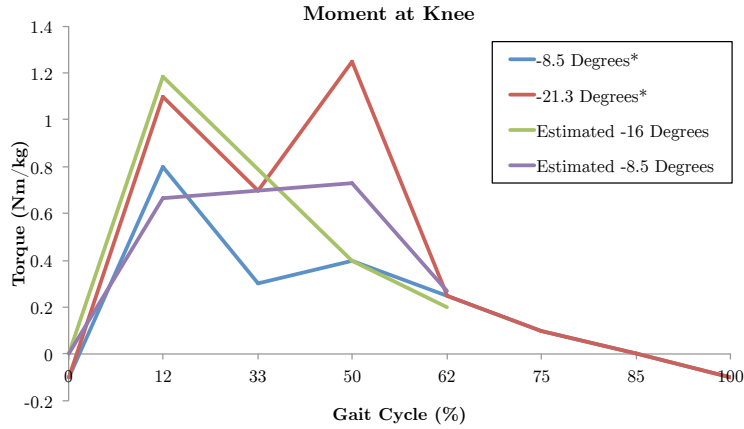


Figure 2-6: Knee moment from free body diagram estimations compared with data from the literature* [10].

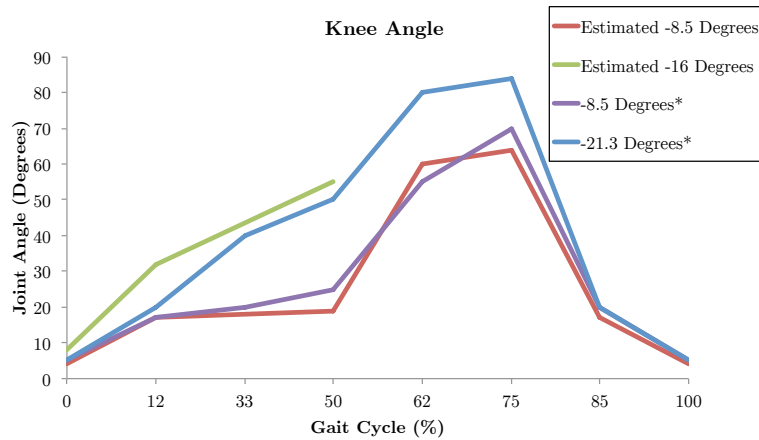


Figure 2-7: Knee angle from free body diagram estimations compared with data from the literature* [10].

The plot in figure 2-6 shows the estimated knee moments from the model plotted

against the calculated knee moments for -8.5 degrees (-15%) and -21.3 degrees (-39%) [10]. As seen in the plot, the moments calculated from the model are within the same range as those recorded in the literature. Because the free body diagram makes the assumption that the body is static, it is not surprising that the measured torque on the knee during walking differs from this assumption. Furthermore, the free body diagram model did not take into account the increased ground reaction forces generated during walking, and it assumed the leg is massless.

The knee angles measured during the biomechanical analysis were then compared to knee angles measured in biomechanical literature [10]. The plot shown in 2-7 shows that the joint angles measured closely match the joint angles presented in the literature. This plot validates that the recorded gait pattern closely matches with the subjects analyzed in the literature [10]. Because of the similarities between knee joint angle measured in the analysis and in the literature review, the knee joint moment data presented in the literature will be used in order to determine functional requirements for the device.

2.3 Functional Requirements

Functional Requirement	Design Specification	Rational
Torque	12 Nm	Decrease torque on knee by 1/5
Weight on Leg	<2.5 kg	Limit amount of weight on extremities
Total weight	<4 kg	Limit total weight
Profile	<5 cm away from leg	Convenient to wear
Walking Speed	0.5 m/s - 1.5 m/s	Adapt to range of natural walking speeds
Control	0% - 62%	Engage during stance phase of walking
Safety	Safe	Safe to use
Comfort	Comfortable	Comfortable to wear for extended periods
Cost	<\$500	Affordable for target population

Table 2.1: Functional Requirements

The user needs survey, prior art search, and biomechanics review led to the development of the functional requirements outlined in table 2.1. The most critical requirement is that the device must provide a resistive torque at the knee during downhill walking. On a -21 degree slope, the peak torque experienced at the knee is

$1.1 \frac{Nm}{kg}$ [10]. In order to compete with existing devices, this device aims to reduce the amount of torque on the users knee by 20%. For a 58 kg individual, the target torque is calculated in equation 2.2. Figure 2-8 shows the relationship between slope angle and peak torque on the knee. In order to determine the function requirements for the device, an upper bound of $1.1 \frac{Nm}{kg}$ was considered. However, peak joint torque on the knee decreases on more gradual slopes (figure 2-8), changing the percentage of total torque that the device is generating.

$$Target\ torque = 1.1 \frac{Nm}{kg} \times 58\ kg \times 20\% = 12\ Nm \quad (2.2)$$

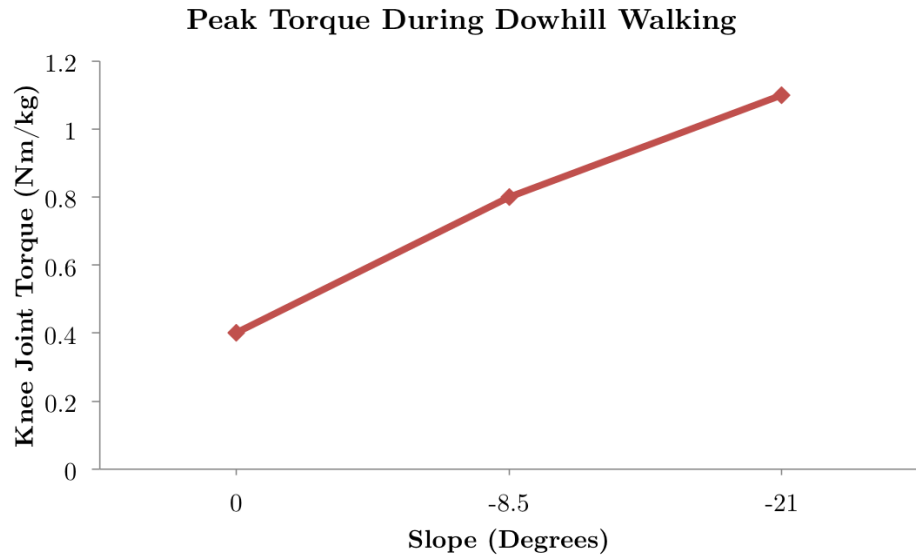


Figure 2-8: Peak torque on knee during downhill walking, at slopes 0, -8.5, and -21 degrees [10].

In order to provide a greater amount of assistance and to be less metabolically costly, the device must also be lightweight. Metabolic rate during walking increases as loads become more distal (figure 2-9), so this project aims to limit the amount of weight added to extremities [12]. For example, a 4 kg load attached to the foot increases metabolic rate by 28% more than the same load attached at the waist (figure 2-9). Therefore, the target weight for the device is less than a 2.5 kg load on the legs, and less than 4 kg of total weight.

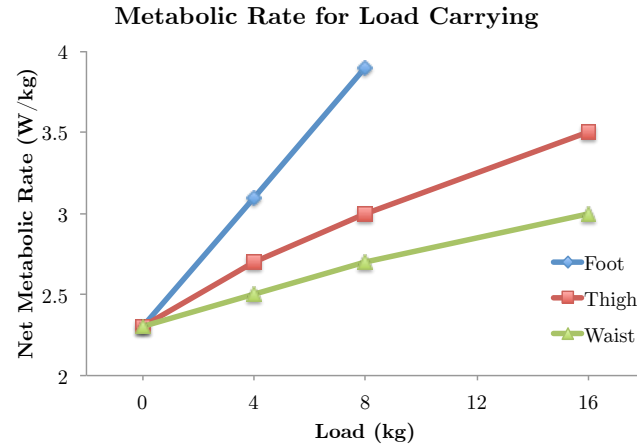


Figure 2-9: Metabolic rate vs. load, as a given load is moved more distally on the body, the metabolic cost of carrying it increases (adapted from [12]).

Additional requirements include that the device must be low profile, so that hiking clothes can be worn under the exoskeleton, it must adapt to a range of normal walking speeds, and it must provide assistance during the stance phase of walking, from 0 to 62% of the gait cycle, while not interfering with swing phase. The device must also be comfortable, safe, and low cost.

Chapter 3

Design

3.1 Design Development

Design concepts were developed according to the functional requirements outlined in table 2.1. Three of the final concepts were selected from a large number of initial designs, and are outlined in this section; a carbon fiber leaf spring (figure 3-1a), torsional spring (figure 3-1b), and an air spring (figure 3-1c).

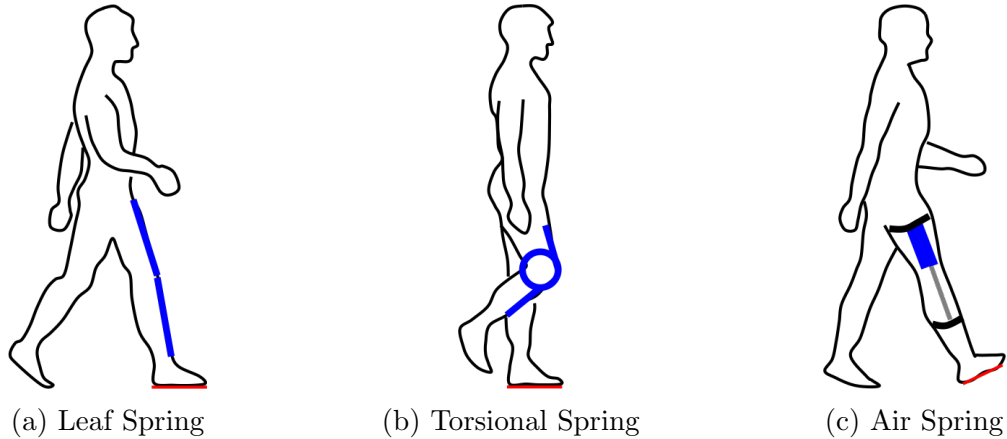


Figure 3-1: Developed design concepts.

3.1.1 Concept 1: Leaf Spring

The leaf spring design (figure 3-1a) consists of carbon fiber sheets that act as springs, providing a resistive torque at the knee that increases in magnitude as knee flex-

ion occurs. Several devices have previously implemented a carbon fiber leaf spring approach in order to generate a torque about the knee (figure 3-2).

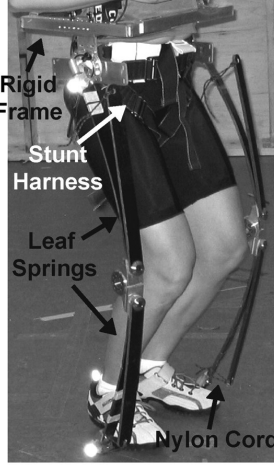


Figure 3-2: Leaf spring design implemented device that uses the recoil from the springs to augment human hopping [13].

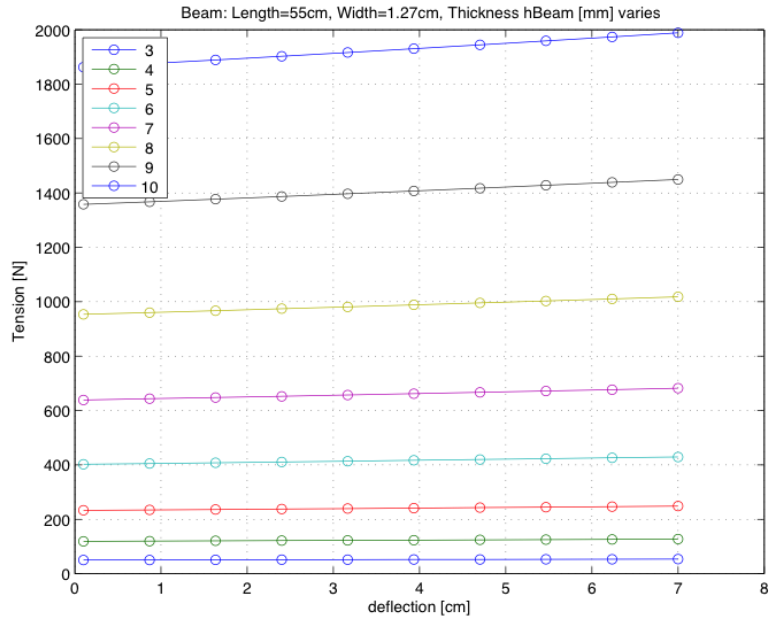


Figure 3-3: Assuming an attachment point of 15 cm below the knee, a force of approximately 130 N is required to produce the torque requirement of 12 Nm. For a leaf spring 55 cm long and 1.27 cm wide, a thickness of 5 mm to generate the required force [14].

In order to determine approximate required dimensions of the leaf springs, a MATLAB script [14] was used to calculate the deflection and force produced using carbon

fiber beams of different dimensions. With an attachment point of 15 centimeters below the knee, a force of approximately 130 N is required to produce the torque requirement of 12 Nm. Figure 3-3 shows that for a beam 55 cm long and 1.27 cm wide, a beam thickness of 5 mm is necessary in order to provide over 130 N of force throughout the range of deflection. These calculations determined that in order to produce the required torque, the carbon fiber leaf spring model would not fulfil the low profile functional requirement. Drawbacks of this design include a bulky form factor, interference between the knees, and strong recoil when the leaf springs are unclutched.

3.1.2 Concept 2: Torsional Spring

The torsional spring concept (figure 3-1b) consists of a torsional spring and a clutching mechanism mounted on the user's knee. This design uses a torsional spring to provide a resistive torque to the knee. First order calculations were performed in order to analyze the feasibility of this design. Using equation 3.1 it was determined that a stainless steel wire would require a wire diameter of 2.1 cm and coil diameter of 4 cm in order to produce the required torque of 12 Nm. This spring size is very large and bulky to be attached to the knee. This size spring would add 1.4 kg to the legs from the spring alone, making the functional requirement of less than 2.5 kg on the legs very difficult when the clutching mechanism and attachment method are taken into consideration.

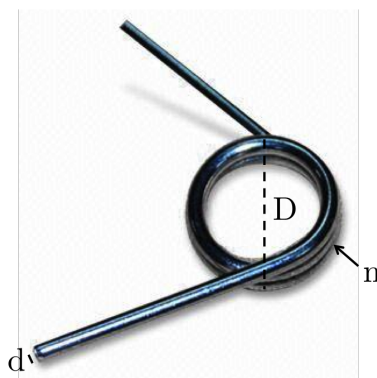


Figure 3-4: Torsional Spring, showing parameters used in equation 3.1, where: D = coil diameter, d = wire diameter, and n = number of coils.

$$k = E \times d^4 \times \pi \div (64,180 \times D \times n) \quad (3.1)$$

Where: E = Shear modulus of material,

d = Wire diameter,

D = Coil diameter,

n = Number of coils.

3.1.3 Concept 3: Air Spring

The air spring design (figure 3-1c) uses compressed air to generate a resistive torque, acting with spring-like behavior to resist compression. In order to determine the force profile of an ideal air spring, equation 3.2 was used to generate the theoretical force profile of the air spring (figure 3-6). Figure 3-6 shows a translated hyperbolic relationship between the compression of the air spring and the force of its resistance, with a vertical asymptote at the total length of the air spring. While this relationship is non-linear, it behaves approximately linearly in the range of compression that occurs during stance, highlighted in red (approximately 0 to 4.3 cm of compression).

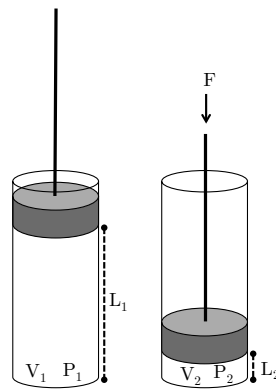


Figure 3-5: Air spring diagram, showing parameters used in equation 3.2, Where: P_1 = initial pressure (atmospheric pressure), P_2 = pressure when compressed, L_1 = initial length of air spring, L_2 = compressed length of air spring, A = area of piston, F = force required to depress piston.

$$P_1 \times V_1 = P_2 \times V_2 \quad (3.2)$$

$$P_1 \times (L_1 \times A) = P_2 \times (L_2 \times A)$$

$$P_2 = P_1 \times \frac{L_1}{L_2}$$

$$F = (P_2 - P_1) \times A$$

Where: P_1 = Atmospheric pressure,

P_2 = Pressure when compressed,

L_1 = Initial length of air spring,

L_2 = Compressed length of air spring,

A = Area of piston,

F = Force

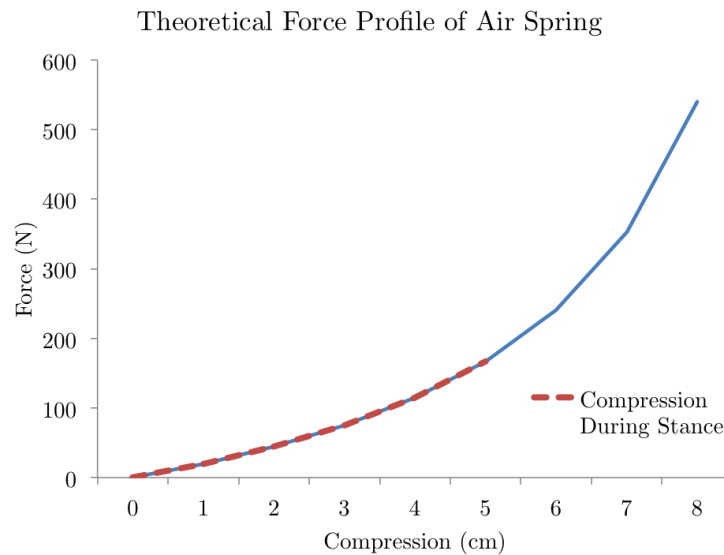
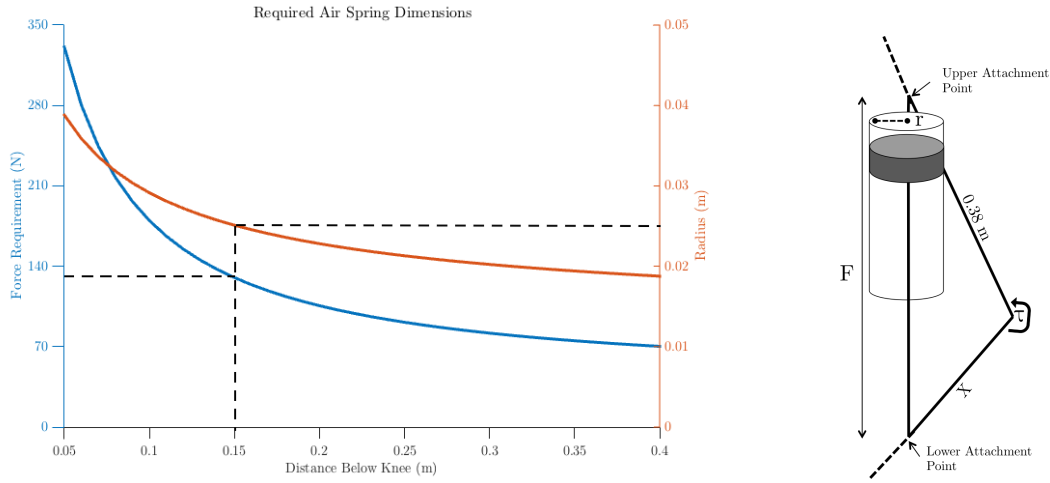


Figure 3-6: Theoretical force profile of air spring over entire length of compression. Red highlights the amount of compression that occurs during stance phase (approximately 4.3 cm).

While determining the required dimensions of the air spring, many variables were considered. A MATLAB model was created in order to model the required attach-

ment, radius, and force requirement for the air spring (figure 3-7a). The upper attachment on the thigh was fixed at 38 cm above the knee, and the attachment distance below the knee was varied (figure 3-7b). The radius of the cylinder is directly related to the amount of resistive force that will be produced when compressed. From this model, it was determined that by using a piston with a radius of 2.5 cm, an attachment point of 15 cm below knee is required. Using this attachment point a force of 130 N is required to produce the required 12 Nm of torque.



(a) MATLAB model, attachment point of 0.15 m below knee is required, with a radius of .025 m and a force of 130 N to generate required 12 Nm of torque.

(b) Model parameters: F = force, r = radius, τ = torque, X = distance below knee.

Figure 3-7: Determining air spring attachment, force requirement, and piston radius.

3.1.4 Design Selection

Each of the three design concepts were evaluated using the Pugh matrix shown in table 3.1. Each design was ranked using 7 different design criteria compared to a neutral datum, a commercially available passive knee brace. Each criteria was weighted from 1 to 5 based on its priority for the overall design. Each design option is then ranked +, -, or 0, depending on if it is better than, worse, or equivalent to the datum, respectively. The sums of the design criteria are then compared to determine the most promising design concept. Pugh analysis informs the air spring design to be

Criteria	Weight	Datum	Leaf Spring	Torsional Spring	Air Spring
Provides Resistive torque	5	0	+	+	+
Lightweight	4	0	0	0	0
Comfortable	3	0	-	+	+
Low Profile	2	0	-	+	0
Adaptable walking speed	3	0	0	-	+
Engage/disengage	4	0	-	-	+
Inexpensive	1	0	0	0	0
+		0	5	10	15
0		0	8	5	7
-		0	9	7	0
Total		0	-4	3	15

Table 3.1: Pugh matrix comparing the leaf spring, torsional spring, and air spring concepts. Each concept is ranked against a neutral datum (passive knee brace) for 7 different criteria [15].

the best approach, receiving positive or neutral rankings for each criteria. Because the torque producing mechanism uses compressed air to generate force, this strategy is able to generate high torques while remaining lightweight. Furthermore, because the clutching mechanism used to engage and disengage the air spring will consist of a valve, it will be possible to attach the control and clutching mechanisms to the users waist rather than on the leg, where extra weight is more metabolically costly. This valve clutching mechanism would also achieve the adaptable walking speed criteria,

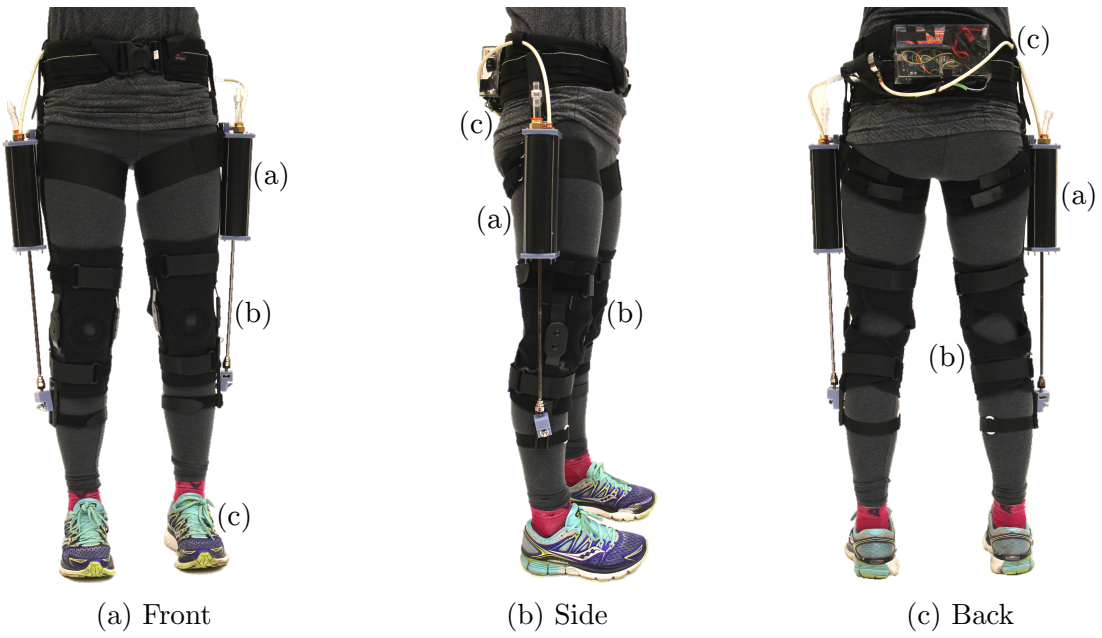


Figure 3-8: Final design overview: (a) air spring, (b) interface, (c) sensing and control.

due to available valves with fast response times, and it is able to provide minimal resistance during the swing phase. The air spring design is therefore capable of meeting the functional requirements outlined in table 2.1 and is the pursued design approach.

3.2 Final Design

The final design (figure 3-8) consists of 3 main modules: an air spring exoskeleton that provides a resistive torque at the knee, a wearable interface to comfortably attach the device to the body, and an integrated sensing and control system to detect the users gait and control the device accordingly.

3.2.1 Air Spring

The air spring is the most critical module of the design (figure 3-9). By resisting compression when sealed on one end, the air spring generates a resistive torque about the knee. A glass cylinder with a graphite piston (figure 3-9b) was used to create the air spring [16]. While a required radius of 2.5 cm and length of 11 cm was calculated (section 3.1.3), due to available stock and budgeting constraints an air spring with radius 2.2 cm and length of 15 cm was used for the prototype. A steel rod was

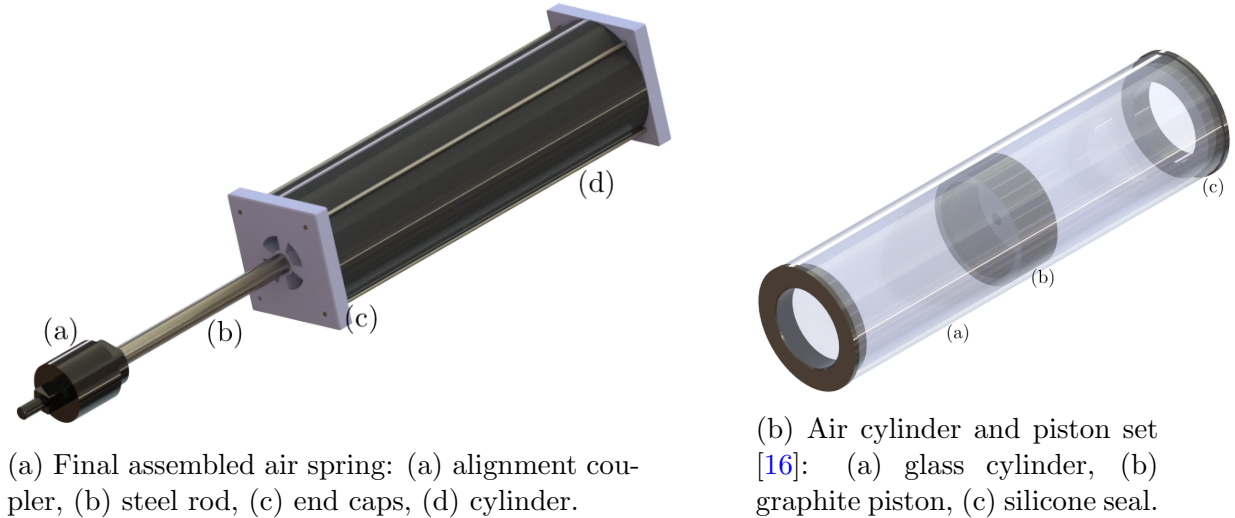
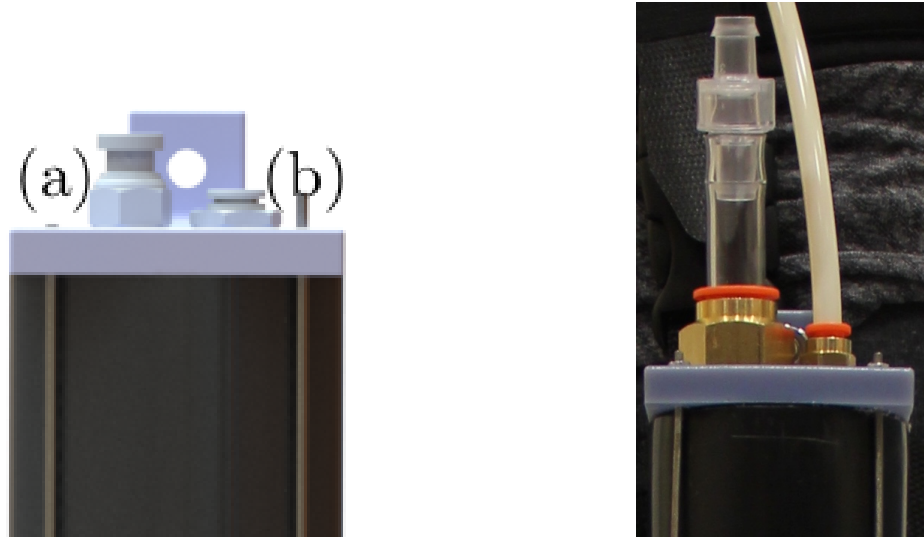


Figure 3-9: Air spring: final assembly (a), and inner glass cylinder (b).

machined to a custom shape, allowing for secure air tight attachment to the piston. A protective PVC cylinder was added around the glass cylinder to add protection from shattering. Custom end caps were designed and 3D printed (drawings in appendix C), sealing the air spring with an air-tight seal on one end. An alignment coupler was added to the end of the rod, to ensure the rod and piston travel straight within the cylinder.



(a) Rendering showing one way valve (a) and control valve (b).

(b) Photo of final valves on assembled air spring.

Figure 3-10: Valves on the end of the air spring allow for control of air flow. Allowing air to flow in during swing but blocking air from exiting during stance is the fundamental mechanism behind the control of the air spring.

There are two valves on the top of the air spring to allow for control of air flow (figure 3-10). The first valve (figure 3-10a(a)) is a one way check valve, that allows air to enter the air spring during extension (swing phase), while not allowing air to exit during compression. A high flow check valve with a low cracking pressure (0.062 PSI) was used, allowing air to enter the air spring with minimal extension force from the knee [17]. This reduces the amount of resistance on the user during knee extention during swing. The second valve (figure (3-10a(b))) is connected to a solenoid valve on the control system. This control valve is closed during stance to provide a resistive torque, and open during swing to not interfere with the natural gait (figure 3-15). The control valve is described in further detail in section 3.2.3.

The air spring is attached by a pin joint to laser-cut delrin attachment plates on the interface on the hip and below the knee. The attachment plates were designed in order to securely hold the air spring in place, which remaining comfortable to the wearer as an integrated component to the soft interface.

3.2.2 Interface

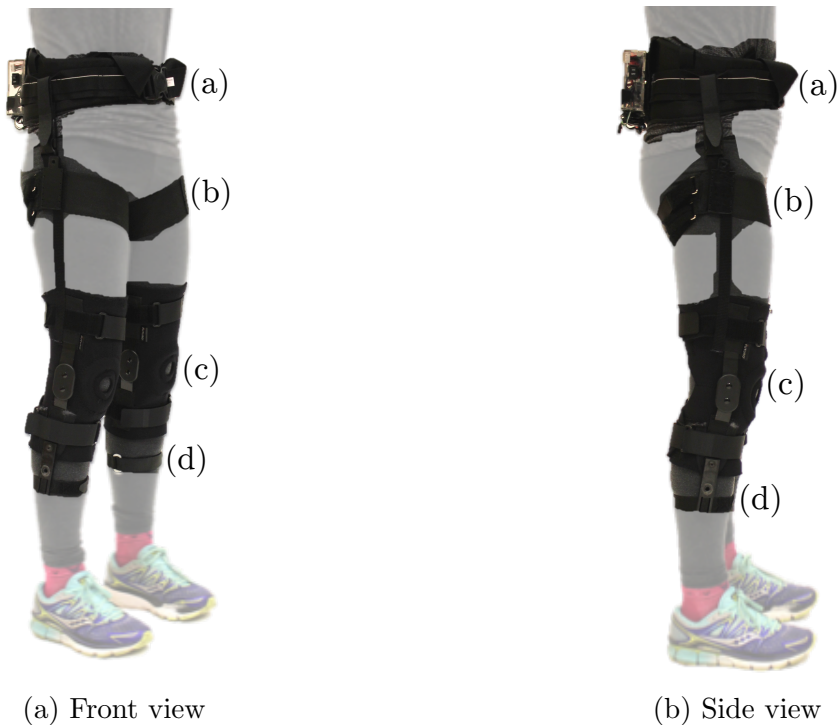


Figure 3-11: Human device interface: (a) waist band, (b) hip strap, (c) knee brace, (d) calf reinforcement band.

The forces on the attachment points of the air spring are large, and the interface must also be secure so that forces are transmitted efficiently from the air spring to the knee without excessive motion. It must be comfortable to the user and not overly constraining so it does not alter the natural gait. The interface was designed using a commercially available knee brace modified for use in this device. A Futuro Sport [2] hinged knee brace was purchased and adapted for use in the exoskeleton. This brace has a rigid hinge on each side of the knee, making it ideal for the rigid to soft transition required for attaching the air spring. The brace is adjustable to a wide

range of sizes, allowing for use on different sized wearers. A commercially available waist band [18] and custom designed hip strap and calf reinforcement band were added to the design to secure attachment. The waist band is worn to help hold the hip straps up, removing some of the forces on the user's body from the hip straps. The waist band is also used to hold the control system components, in an effort to reduce weight attached to the users legs. The hip strap holds the air spring in place on the users thigh. This strap has a laser-cut rigid attachment plate integrated into the soft fabric Velcro band. While the strap must be tight enough to hold the air spring in place, it must not be overly restrictive to the users movement.

3.2.3 Sensing and Control

The sensing system consists of a foot switch in each shoe connected to an Arduino microcontroller. When heel strike is detected by the foot switches, the signal is passed to the microcontroller and the valve is controlled appropriately (figure 3-12). These foot switches fit comfortably in the users shoe and are able to accurately detect heel strike while walking on a variety of slopes and terrain (figure 3-13).

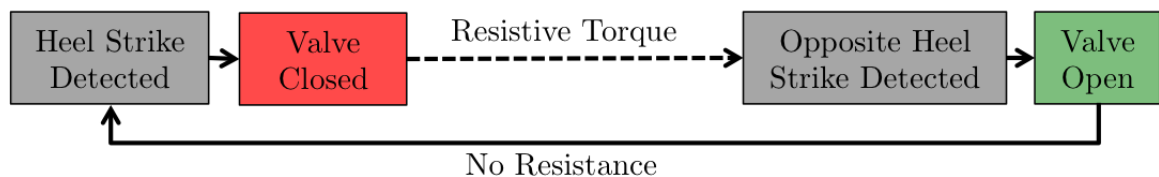


Figure 3-12: Device control: when heel strike detected control valve is closed, generating a resistive torque about the knee during stance phase. When opposite heel strike detected, control valve opened.



Figure 3-13: Foot switches are worn in the user's shoes to detect heel strike [19].

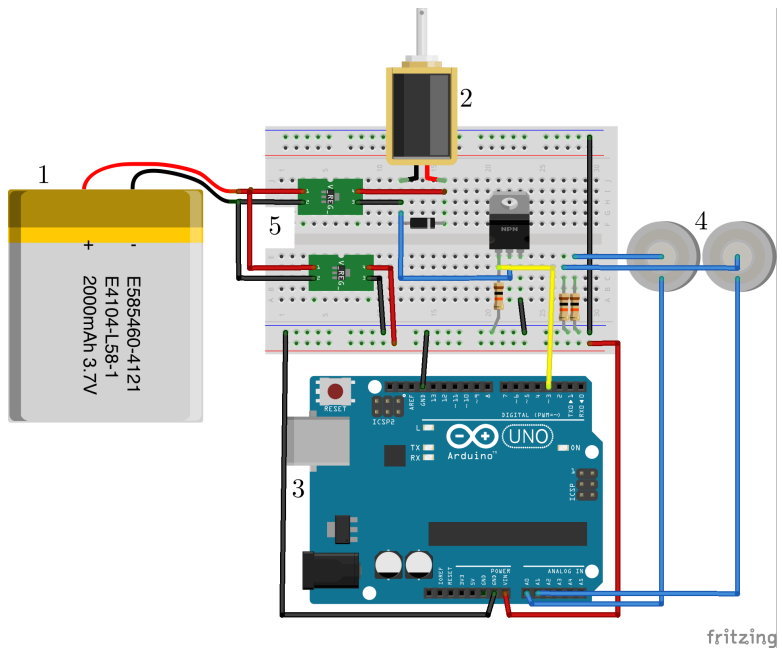


Figure 3-14: Electronic control circuit: 1. lithium polymer battery, 2. solenoid valve, 3. Arduino microcontroller, 4. foot switches, 5. voltage regulators.

An Arduino microcontroller regulates a solenoid valve that activates and inactivates the air spring (figure 3-14). The valve is powered by a rechargeable lithium polymer (LiPo) battery and is completely portable. The response time of the valve must allow for the pressure inside the cylinder to be released in less than 250 milliseconds, in order to not interfere with the swing phase of the gait cycle. To determine the necessary valve properties, the required flow coefficient was calculated.

$$C_v = q \times SG \times (T + 460)^{\frac{1}{2}} \div (660 \times p_i) = 0.18 \quad (3.3)$$

Where: C_v = Valve coefficient,

q = Flow rate,

SG = Specific gravity,

T = Temperature,

p_i = Inlet pressure

Therefore, a valve with a flow rating of 0.18 was required (figure 3-15). The device control mechanism allows for the use of a single three-way valve to control air springs on two legs. When the air spring on one leg is closed during stance, the other air spring is open as the opposite leg is in swing.



Figure 3-15: Parker cyclone direct acting solenoid valve [20].

3.3 Design Evolution



Figure 3-16: Design evolution of interface, red arrows show direction of displacement when forces applied from air spring. Modification made (1) waist band to support load, (2) strap between hip band and waist band to prevent sliding down leg, (3) calf reinforcement strap, (4) tension strap between knee brace and hip band.

Figure 3-16 shows the evolution of the interface design. Version 1 of the design (figure 3-16a) consisted of the hip band and knee brace only. Initial tested determined that additional reinforcement was necessary to keep the air spring secured. In version 2 (figure 3-16b), the waist band and calf reinforcement straps were added. However, further testing showed there were still problems with the air spring displacing upwards on the hip during use, and in version 3 (figure 3-16c) a strap connecting the knee brace to hip band was added, which remains under tension while the air spring is engaged, preventing the air spring from sliding upwards.

3.4 Design Evaluation

Following the construction of the device prototype, evaluation of the device mass, force profile, and power consumption were performed in order to analyze performance.

3.4.1 Device Mass

The mass of each component is outlined in table 3.2. From this analysis it is apparent that the functional requirement of total device weight under 4 kg and weight on legs under 2.5 kg has been met.

Components on Waist	Weight (g)	Components on Legs	Weight (g)
Waist Band	347.4	Air Spring (x2)	587
Control Box	360	Interface (x2)	555.5
Solenoid	512.3	Foot Switch (x2)	88.7
Battery	226.4		
Total on Waist	1446.1	Total on Legs	2462.4
		Total Device	3908.5

Table 3.2: Mass of components, separated into components attached to user's waist (1446.1 g), legs (2462.4 g), and total weight (3908.5 g).

3.4.2 Power Requirements

Another functional requirement outlined in table 2.1 is that the device must be portable and suitable for prolonged use. The current design uses a rechargeable LiPo

battery that is capable of outputting 14.8 V and has a rating of 2200 mAh. Equation 3.4 estimates the life of the battery during each charge. The current draw from the battery consists of the Arduino microcontroller and the solenoid valve. Because the valve is only activated 50% of the time, and it draws no current in its passive state, total average current is adjusted. From this calculation it is estimated that the battery will last 4.75 hours between charges. This is more than sufficient run time for a long period of use, such as a full afternoon of hiking. However, due to inefficiencies in the voltage regulators in the circuit, and the fact that the LiPo batteries should not be used until complete discharge, the actual lifetime per charge is less than this best-case calculation.

$$I_{average} = 50\% \times I_{Valve} + I_{Arduino} = 0.5 \times 0.83 A + 0.047 A = 0.46 A \quad (3.4)$$

$$\text{Theoretical Battery Life} = 2.2 \text{ Ah} / 0.46315 \text{ A} = \mathbf{4.75 \text{ hours}}$$

3.4.3 Characterization of Air Spring

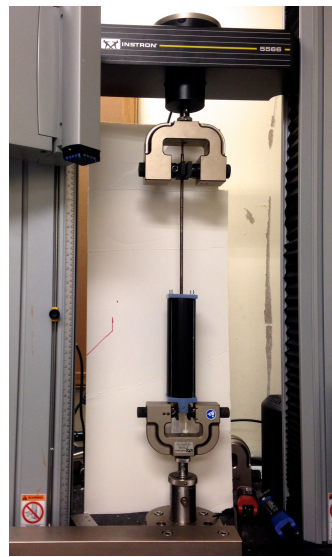


Figure 3-17: Air spring characterization under unilateral compression.

As described in section 2.2, the second peak in joint torque (figure 2-4) is when the knee is at greater risk of fatigue, joint stress, and injury. Therefore, an ideal assistive

device will provide the maximum amount of assistance during the second peak in joint torque, at approximately 50% of the gait cycle. Creating a linear approximation of the torque increase results in a simplified linear model, approximating the knee as a spring-like mechanism. This matches the force profile of an ideal device, providing equivalent assistance throughout the entire stance phase, with the greatest amount of assistance at the end of stance.

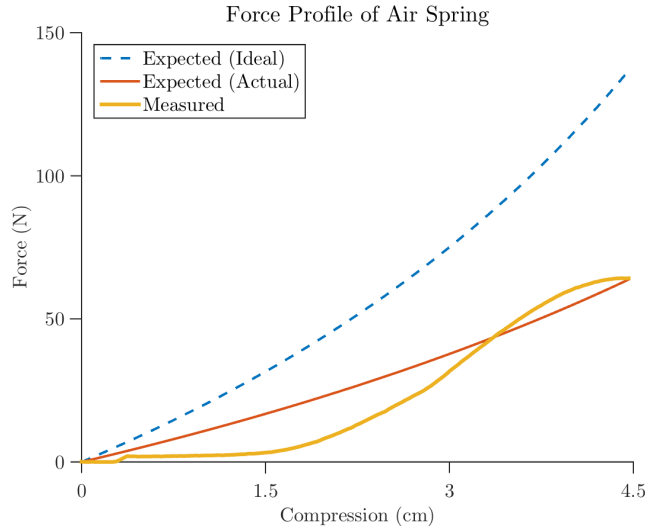


Figure 3-18: Force profile of air spring, results of characterization testing (yellow)(testing shown in figure 3-17), calculated based on ideal dimensions (blue), and calculated based on actual prototype dimensions (red)

In order to quantify the force profile of the airspring, an Intron electromechanical testing machine was used to measure the amount of force required to compress the closed air spring a given distance (figure 3-17). Figure 3-18 demonstrates that the air spring behaves as expected (yellow), producing a force profile that closely matches the calculated force output for the prototype dimensions (red). Although the force output is slightly less than the expected output for an air spring of ideal dimensions, by adjusting the length and radius a higher torque can be produced (figure 3-19). Due to budget and time constraints, ideal dimensions were not achieved during the scope of this project. Because of the discrepancies between ideal and actual air spring dimensions, the device is unable to output the goal torque of 12 Nm, and is in reality generating approximately 5 Nm of torque. Torque output was compared against

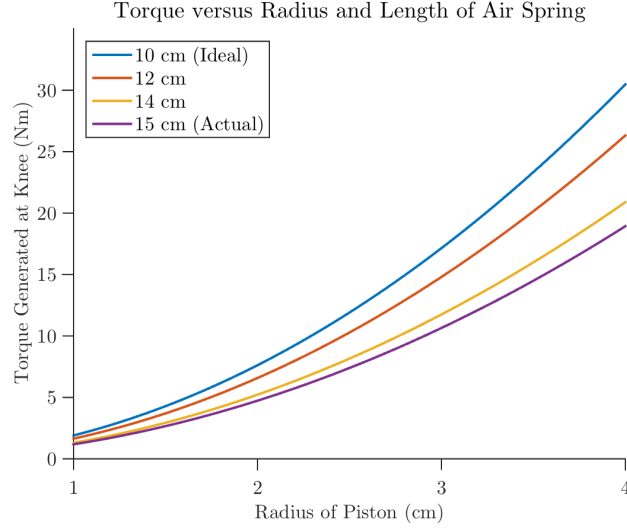


Figure 3-19: Theoretical torque generated by air spring for varied lengths and piston radii. Actual expected torque output (purple) could be increased by decreasing length and increasing radius to the ideal dimensions (blue).

piston radius for four different lengths of air springs (figure 3-19). This analysis demonstrates that by adjusting the dimensions of the glass cylinder and piston used during fabrication, the torque output could be increased in order to achieve the functional requirements. Figure 3-20 demonstrates the relationship between the slope of the walking surface and the amount of torque generated at the knee. Because knee flexion increases for steeper slopes, air spring compression also increases on steeper slopes, thus generating a greater resistive torque. In this way, the air spring device automatically adjusts assistance depending on the steepness of the slope.

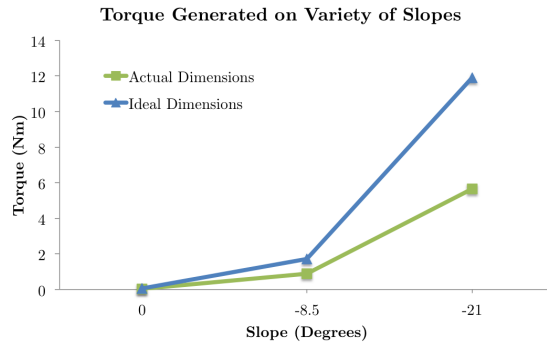


Figure 3-20: Relationship between the slope of the walking surface and the amount of torque generated at the knee.

Chapter 4

Testing and Results

4.1 Human Subject Testing



Figure 4-1: Human subject testing on declined treadmill.

Performance of the device was quantitatively evaluated during human subject testing. Muscle activity of knee extensors (rectus femoris and vastus medialis) was measured using electromyography (EMG) in order to determine if the device was helping alleviate stress on the knee. Activity of the biceps femoris was measured to

analyze the effect on muscles during swing phase. The exoskeleton was tested on one volunteer subject as proof of concept of the effects of the device on downhill walking. Muscle activity, ground reaction forces, and joint angle were measured while walking on a treadmill at 1.0 m/s at variable slopes of 0 degrees, -5 degrees, and -15 degrees. Three conditions were measured at each slope, the device worn in its active state, the device worn in its passive state, and a baseline trial with the device off, for 1 minute each.

Assistive Knee Device Testing Protocol

Data collected	Ground reaction forces, muscle activity, joint angle, Arduino signal
Slopes	Level walking, -5 degrees, -15 degrees
Device states	Device active, device inactive, device off
Speed	1 m/s

Table 4.1: Testing protocol

Trial #	Condition
1	0 degree slope, device inactive
2	0 degree slope, device active
3	-5 degree slope, device inactive
4	-5 degree slope, device active
5	-15 degree slope, device inactive
6	-15 degree slope, device active
7	0 degree slope, device off (control)
8	-5 degree slope, device off (control)
9	-15 degree slope, device off (control)

Table 4.2: Trials measured during testing, each condition measured for 1 minute each while walking on a treadmill at 1 m/s.

Non-invasive EMG surface electrodes were placed on the leg of the healthy adult participant in order to test muscle activation while walking. An off-the-shelf disposable adhesive kit with leads for the EMG electrodes was used (Natus Product 019-414200) as shown in figure 4-2. Analysis of the EMG data was performed to determine the effect that the device has on muscle activation.

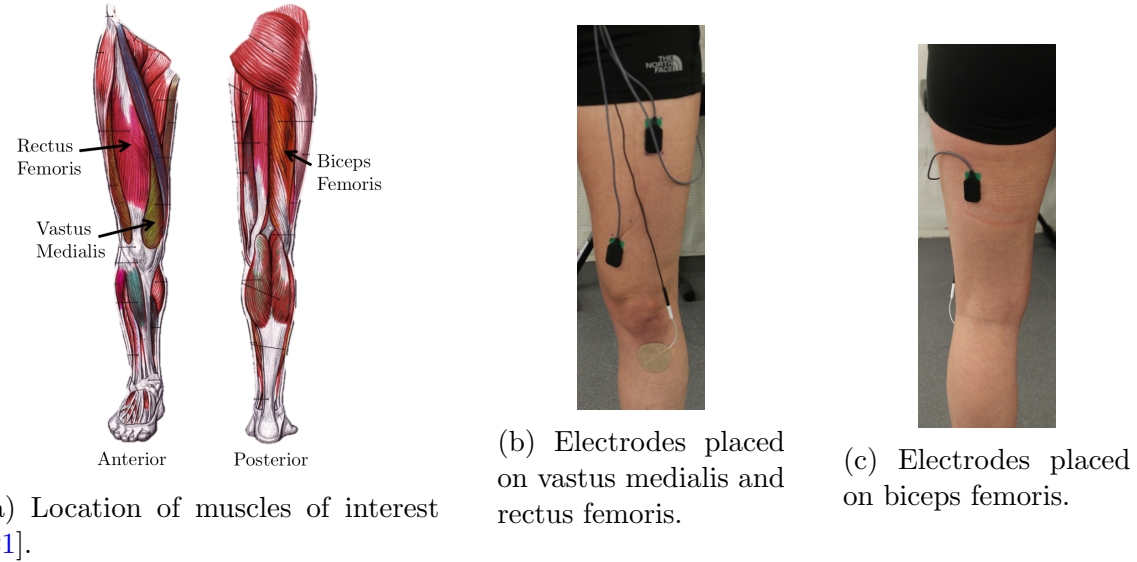


Figure 4-2: Electrode placement during human subject testing.

4.2 Analysis

The EMG and GRF data was processed in Visual 3D using a processing algorithm developed by members of the Harvard Biodesign Lab. The EMG data was filtered using a bandpass with a highpass cutoff frequency of 10 hertz, and a low pass cutoff frequency of 450 hertz. The data was then rectified and passed through a second lowpass filter, with a 6 hertz cutoff frequency. The last 10 strides of each 1 minute trial were segmented and averaged over the gait cycle.

4.3 Results

Results from testing on the -5 degree slope are shown in the body of the report (additional results in Appendix A).

Figures 4-3 and 4-4 show muscle activity for vastus medialis and rectus femoris averaged from 10 strides over the entire gait cycle. Muscle activity for the inactive device is plotted in orange, and active in blue. The red dotted line is the portion of the gait cycle during which the air spring is providing a resistive torque. From this data we see that there is a decrease in peak muscle activity for both the vastus medialis and rectus femoris.

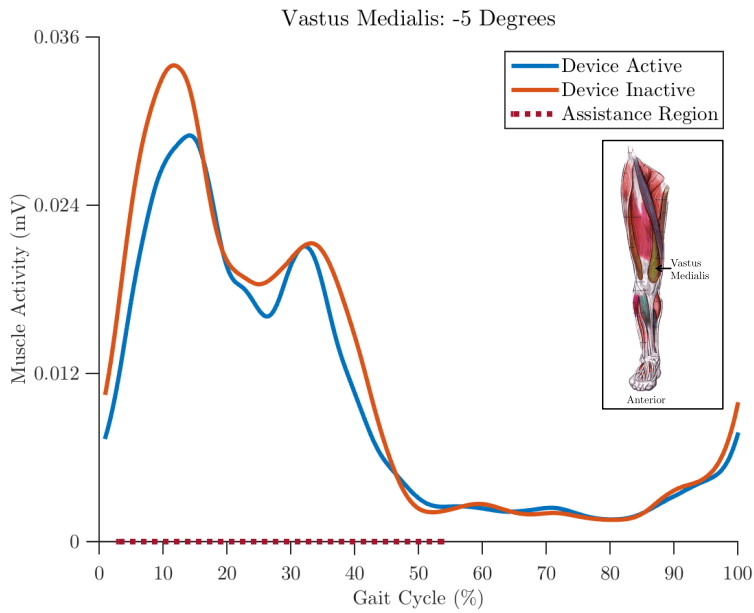


Figure 4-3: Vastus medialis muscle activity data on -5 degree slope (average of 10 strides).

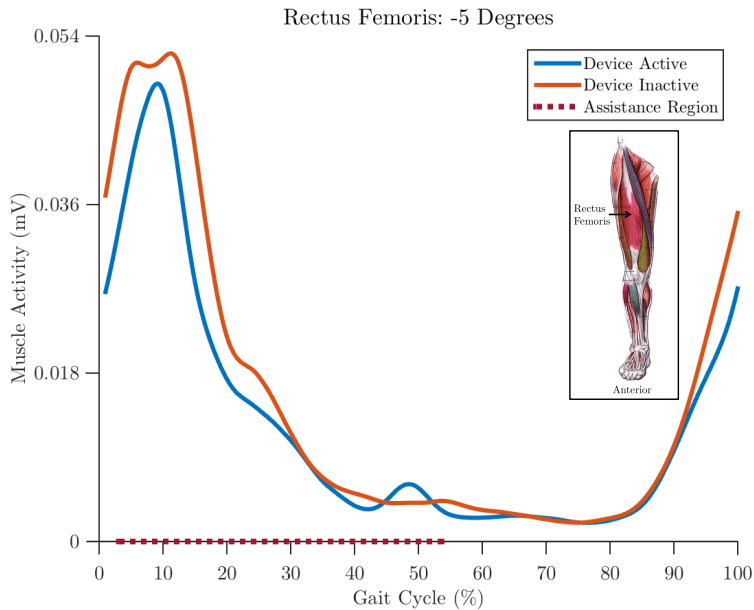


Figure 4-4: Rectus femoris muscle activity data on -5 degree slope (average of 10 strides).

The muscle activity was then integrated over the entire gait cycle, to determine the overall affect the device has on walking. The vastus medialis shows a statistically significant 11.9% decrease in muscle activity (figure 4-5), and the rectus femoris

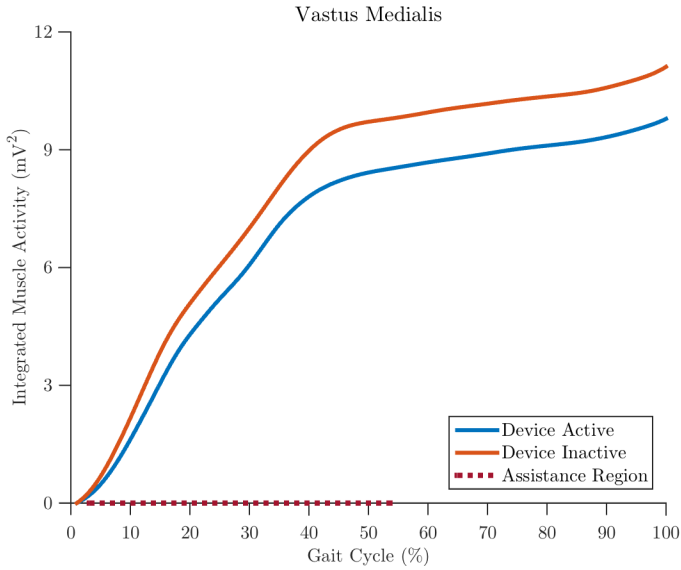


Figure 4-5: Vastus medialis muscle activity integrated over entire gait cycle (average of 10 strides). An 11.9% decrease in total vastus medialis muscle activity between the inactive (11.11 ± 0.75), and active (9.79 ± 1.16) trials was shown, $t(18) = -3.0411$ $p = 0.007$.

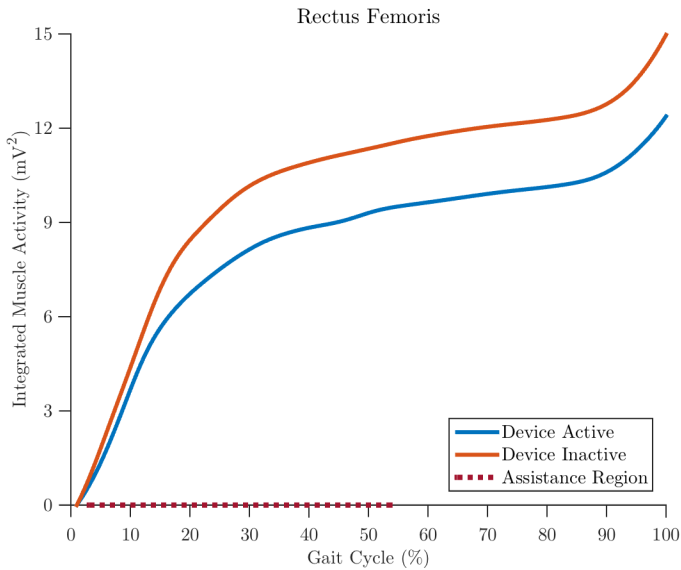


Figure 4-6: Rectus femoris muscle activity integrated over entire gait cycle (average of 10 strides). A -17.3% decrease in total rectus femoris muscle activity between the inactive (14.97 ± 2.82), and active (12.38 ± 1.95) trials was shown, $t(18) = -2.389$ $p = 0.028$.

shows a statistically significant 17.3% decrease (figure 4-6). There was a statistically significant decrease (-11.9%) in the total vastus medialis muscle activity between the

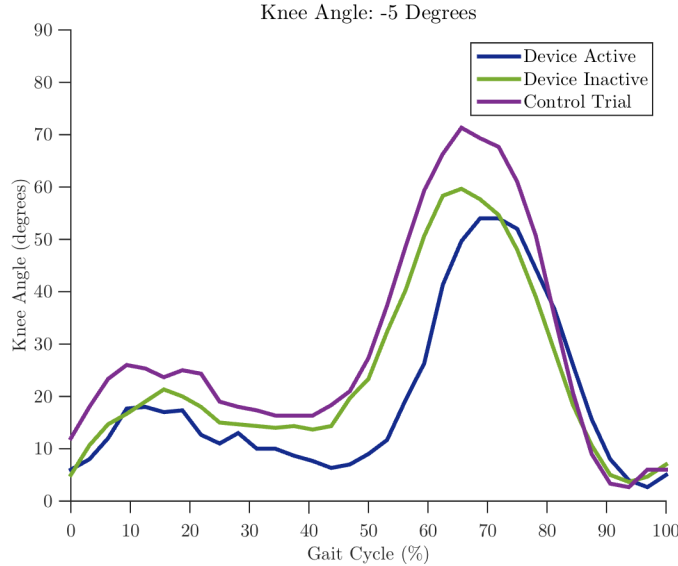


Figure 4-7: Joint angle measured on -5 degree slope. Analyzed using image analysis software [9].

inactive (11.11 ± 0.75), and active (9.79 ± 1.16) trials, $t(18) = -3.0411$ $p = 0.007$ (figure 4-5). There was also a statistically significant decrease (-17.3%) in the total rectus femoris muscle activity between the inactive (14.97 ± 2.82), and active (12.38 ± 1.95) trials, $t(18) = -2.389$ $p = 0.028$ (figure 4-6). Joint angle was monitored during testing to determine the effect the device has on gait. Comparison of joint angle between trials in which the device was on versus off (figure 4-7) shows that knee flexion during the second half of the gait cycle is slightly lower when the device is on. This implies that the device resists knee flexion during swing slightly, but the overall gait pattern is unaltered. Additionally, no gait abnormalities were visually observed during data collection. This confirms that the device can be used during walking without overly constricting the natural gait.

Chapter 5

Conclusion

5.1 Conclusion

This thesis has described the design, construction, and testing of a novel device for assistance during downhill walking. This device fills the current area of need for semi-active devices. This device improves upon current technologies by designing a device that provides more assistance than passive devices, at a lower cost, weight, and power requirement than active devices. By designing a device that provides a resistive torque of 5 Nm to the wearers knee, it has been possible to decrease torque about the knee by approximately 10% for a 58 kg individual. This thesis will help delay onset of fatigue, reduce muscle strain, and help prevent degenerative joint diseases. This will decrease the prevalence of knee pain and injury, reducing medical costs as well as reducing lost wages due to disability.

Potential users were surveyed as initial research for this thesis, demonstrating that over 75% of the target population expressed interest in using an assistive exoskeleton while hiking downhill. Biomechanics research identified the portion of the gait cycle during which the knee is most susceptible to fatigue and injury. This research led to the development of functional requirements, from which initial design concepts were developed. The developed concepts were evaluated and compared according to their ability to achieve the stated functional requirements, and the proposed air spring design was selected. The final device includes an air spring, interface, and

sensing and control system. Initial device evaluation was performed, showing that the device successfully met the requirements for mass, torque output, and power requirements. Following initial evaluation, human subject testing was conducted in order to determine the effect of the device on muscle activity and gait. Results showed that on a -5 degree slope, the device can reduce muscle activity by up to 17%. Additionally, joint angle data showed that there were no substantial effects on the users natural gait pattern.

In conclusion, by augmenting healthy individuals and assisting physically impaired individuals, this device will help the active, elderly, and physically impaired alike by decreasing muscle fatigue, decreasing risk of overuse injuries, increasing independence, and improving overall quality of life.

5.2 Future Work

Initial testing showed promising results for the designed exoskeleton. Future optimization of the device will include further testing, conducted on healthy as well as physically impaired subjects, reducing the profile and weight of the device, modifying air spring radius and length to match the ideal dimensions outlined in this thesis in order to increase torque output, optimizing the control system for use on a variety of terrain, including indoors and outdoors, and reducing the resistance provided from the interface during swing.

The interface module could be improved in order to reduce the amount of fabric required to effectively attach the air spring to the user without compromising function and comfort. Future improvements to the control system could include using a solenoid valve that is smaller and lighter while maintaining the current response time and pressure ratings. Additionally, a smaller battery would allow the overall weight of the device to be reduced. Customizing the size would require having several different options for the stroke length of the air spring, as individuals with longer legs will require a device that has more room for piston travel.

Acknowledgments

I would like to take this opportunity to thank my advisors, Dónal Holland and Panos Polygerinos, for being incredible mentors throughout this project. Without their guidance this project would not be half of what it is today. Thank you for the huge amount of time you have put into helping me make this project a success. And thank you for always having high expectations, and for believing in my ability to achieve them.

I would also like to thank Conor Walsh for being a great mentor during my past few years at Harvard. Thank you for providing me with the initial idea for this project, and for supporting me through this and other research endeavors.

I would also like to thank the members of the Harvard Biodesign Lab for their assistance throughout the project. Especially Stephen Allen and Fausto Panizzolo for their assistance during the testing and data analysis portions of the project, and Alan Asbeck for his initial guidance during the formation of this project.

I would like to thank my friends for helping me in more ways than they know. From proofreading drafts to providing emotional support during times of frustration, your genuine support and willingness to lend a hand means so much.

Finally, I would like to thank my family for supporting my educational career from the beginning. Thank you instilling in me a passion for learning, and for teaching me that the most important component to success is hard work and dedication.

Appendix A

Additional Testing Results

A.1 Additional EMG Data Plotted by Slope

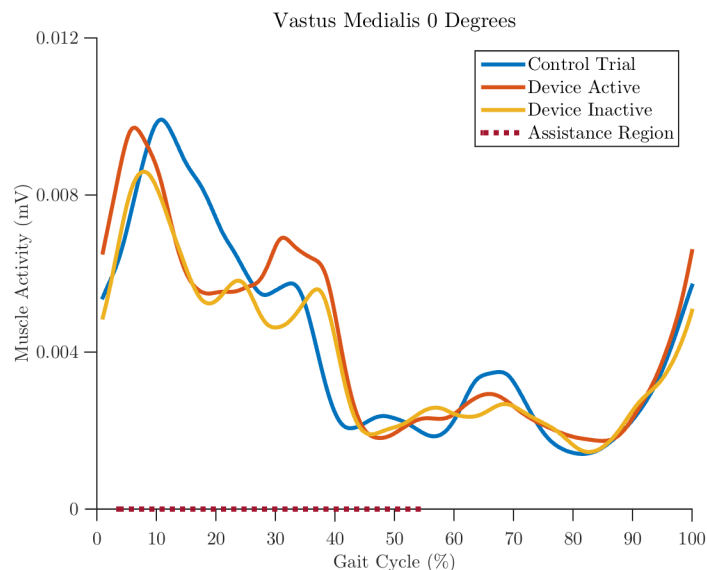


Figure A-1: Vastus medialis 0 degrees

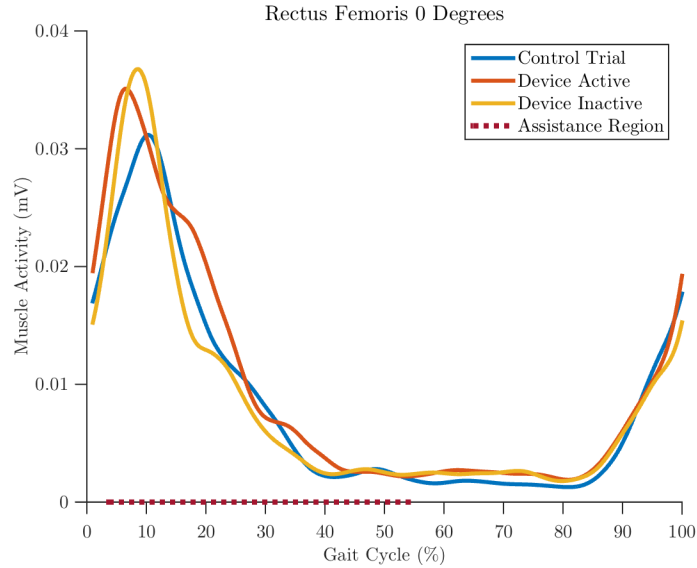


Figure A-2: Rectus femoris 0 degrees

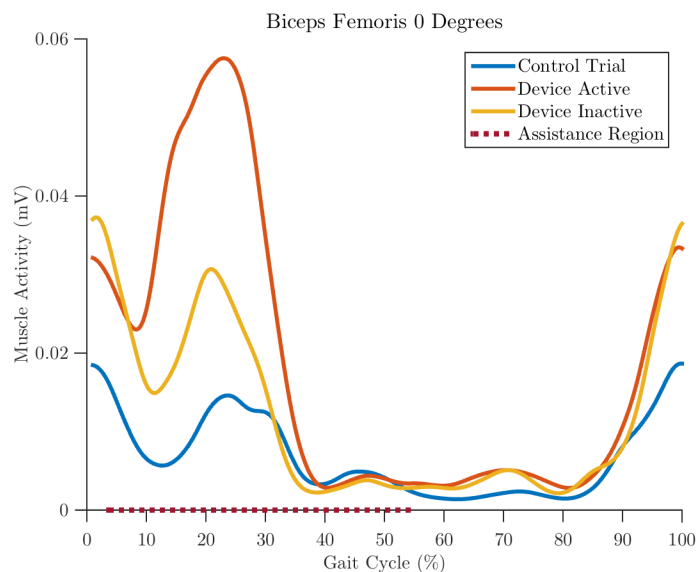


Figure A-3: Biceps femoris 0 degrees

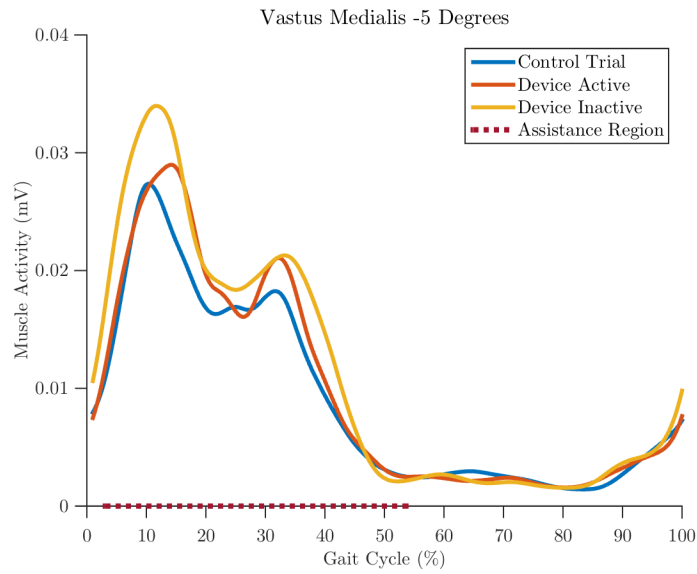


Figure A-4: Vastus medialis -5 degrees

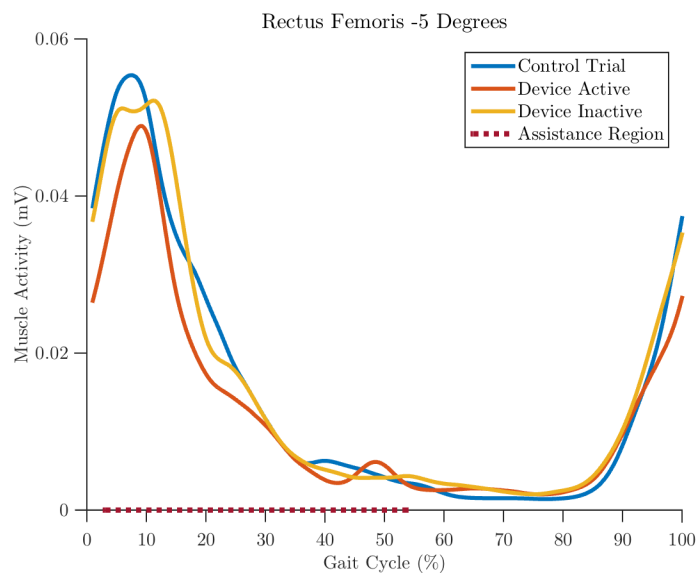


Figure A-5: Rectus femoris -5 degrees

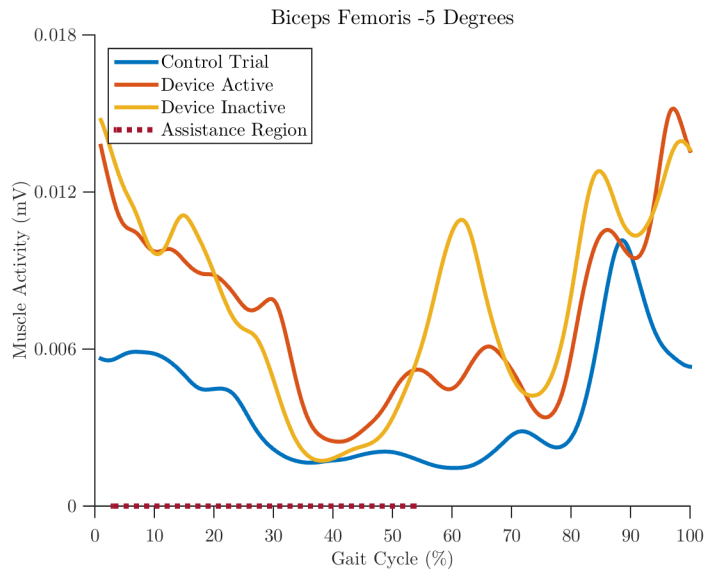


Figure A-6: Biceps femoris -5 degrees

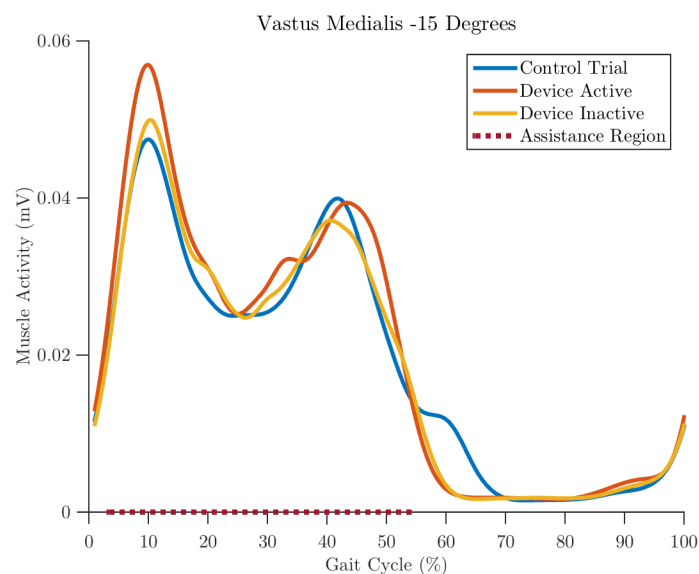


Figure A-7: Vastus medialis -15 degrees

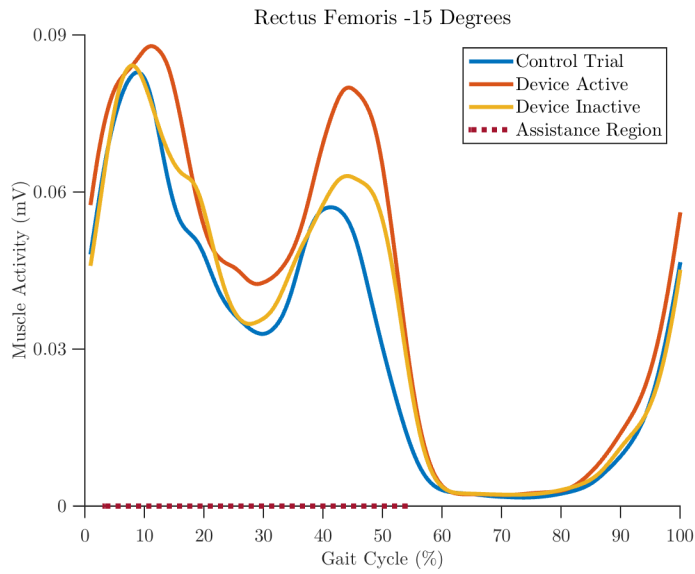


Figure A-8: Rectus femoris -15 degrees

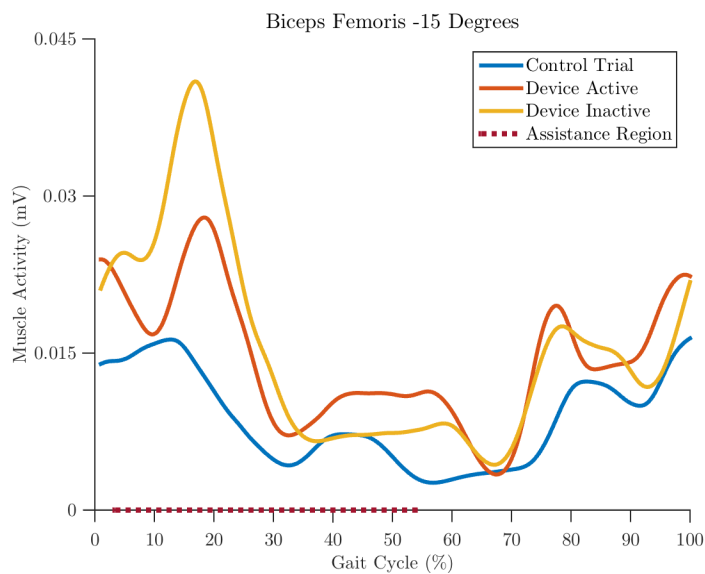


Figure A-9: Biceps femoris -15 degrees

A.2 Muscle Activity and Standard Deviation

Data plotted individually for each muscle at each condition. The grey line is average muscle activity between 10 trials, and the shaded area represents standard deviation.

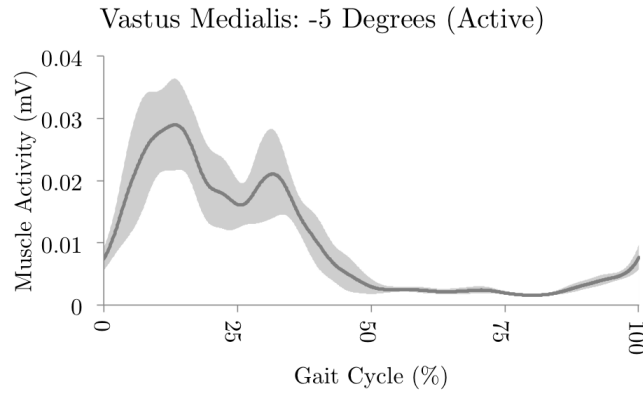


Figure A-10: Vastus medialis -5 degrees active

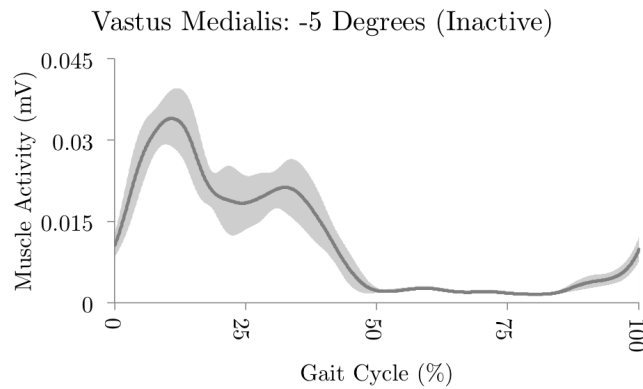


Figure A-11: Vastus medialis -5 degrees inactive

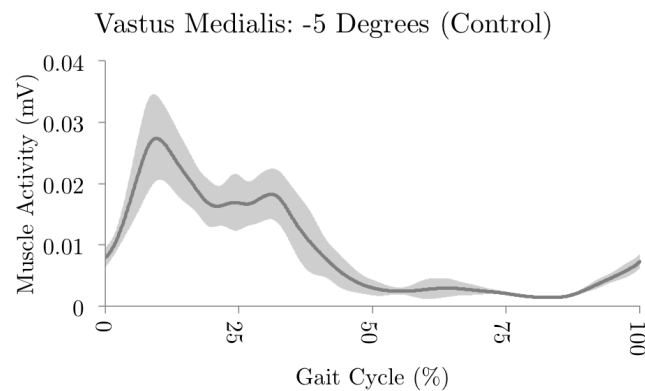


Figure A-12: Vastus medialis -5 degrees control

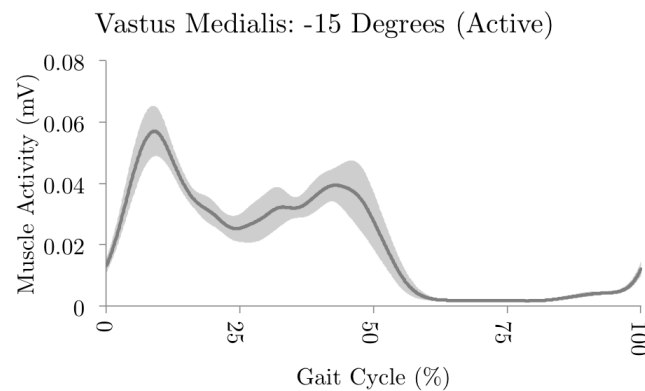


Figure A-13: Vastus medialis -15 degrees active

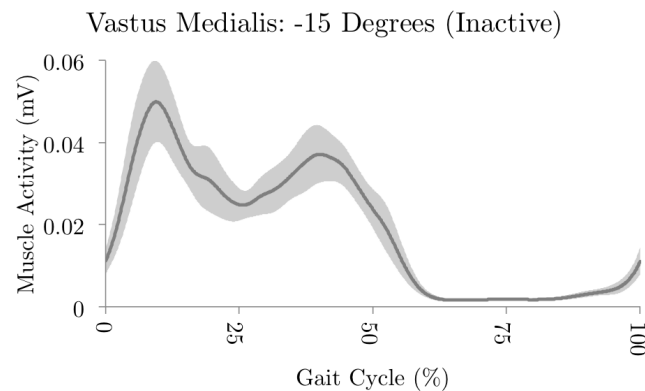


Figure A-14: Vastus medialis -15 degrees inactive

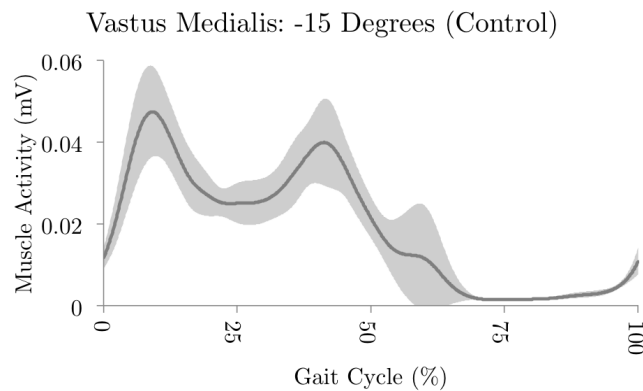


Figure A-15: Vastus medialis -15 degrees control

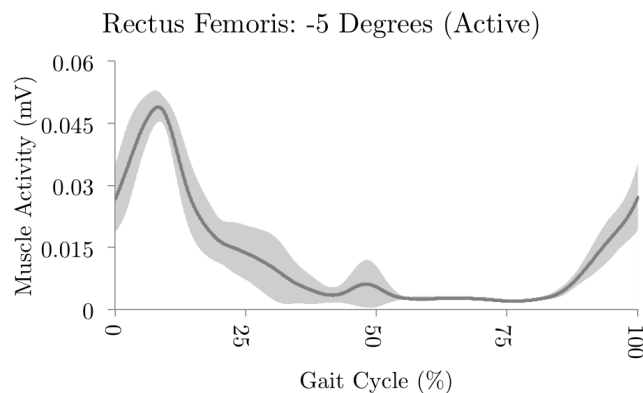


Figure A-16: Rectus femoris -5 degrees active

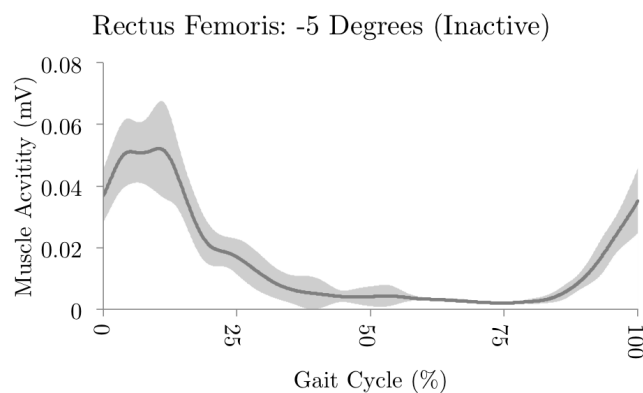


Figure A-17: Rectus femoris -5 degrees inactive

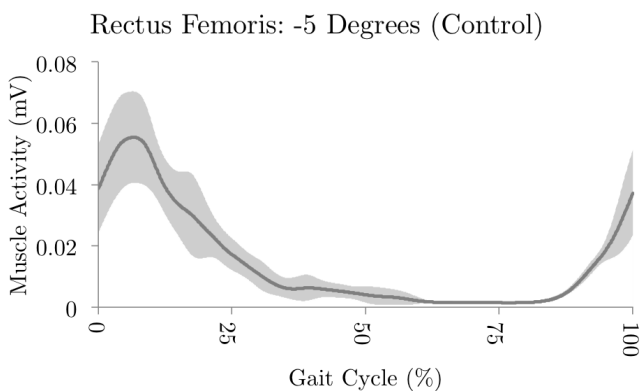


Figure A-18: Rectus femoris -5 degrees control

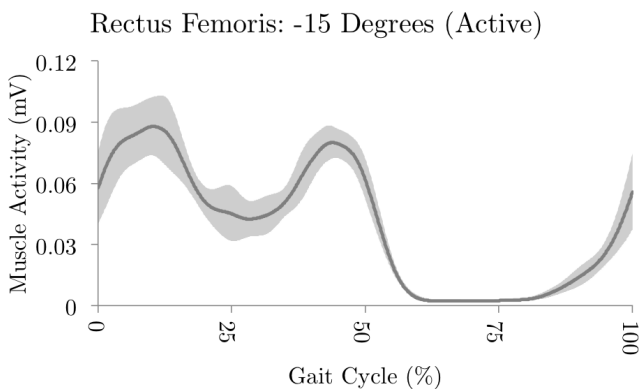


Figure A-19: Rectus femoris -15 degrees active

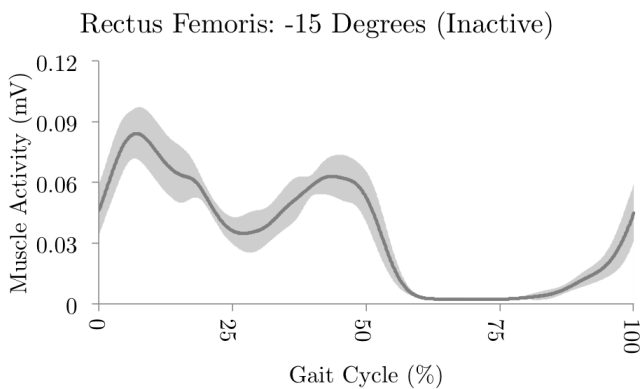


Figure A-20: Rectus femoris -15 degrees inactive

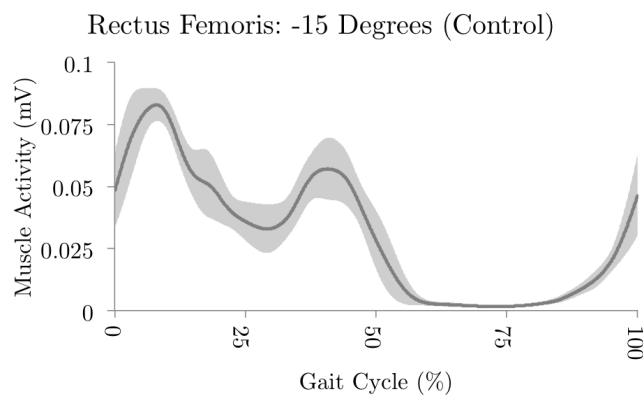


Figure A-21: Rectus femoris -15 degrees control

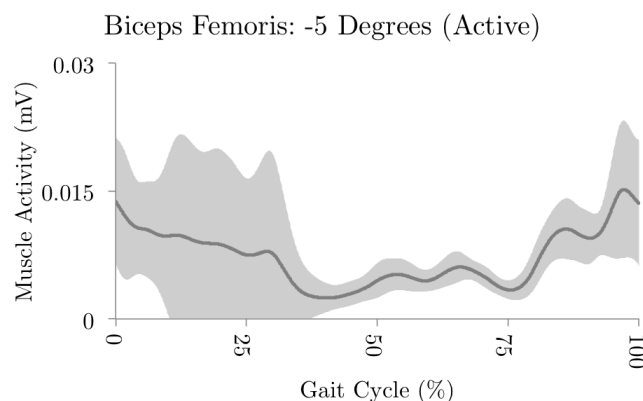


Figure A-22: Biceps femoris -5 degrees active

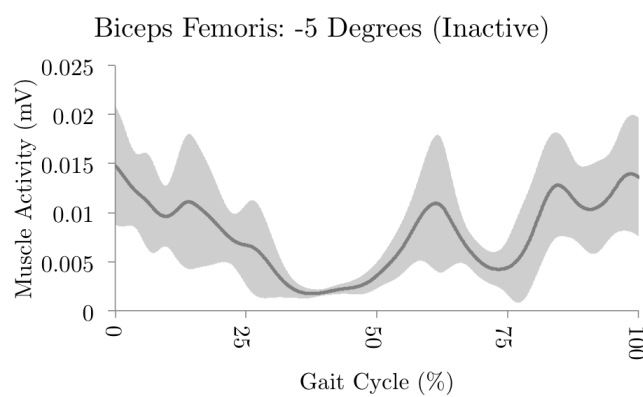


Figure A-23: Biceps femoris -5 degrees inactive

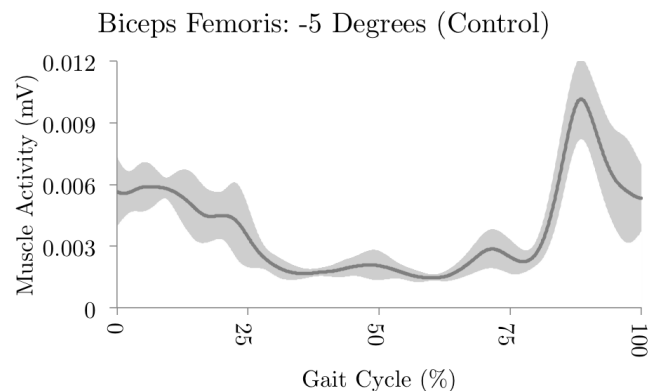


Figure A-24: Biceps femoris -5 degrees control

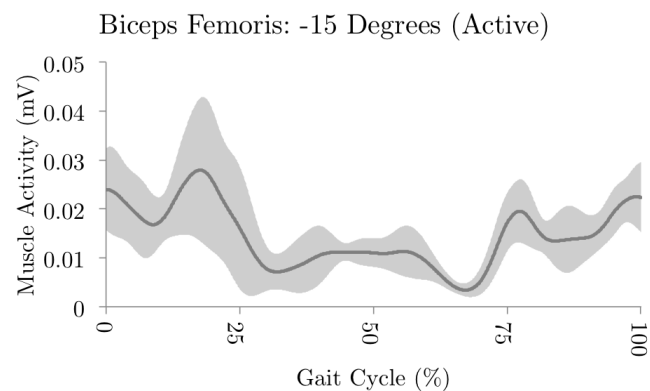


Figure A-25: Biceps femoris -15 degrees active

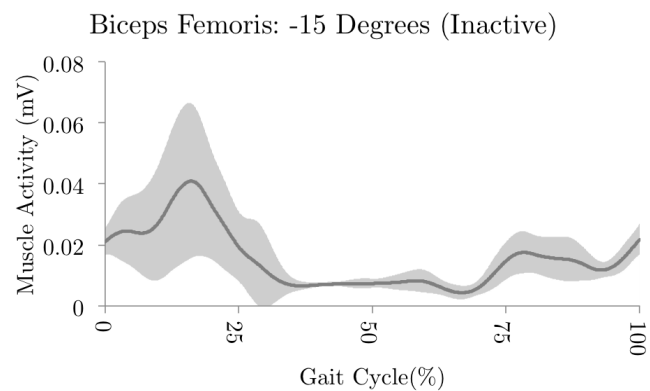


Figure A-26: Biceps femoris -15 degrees inactive

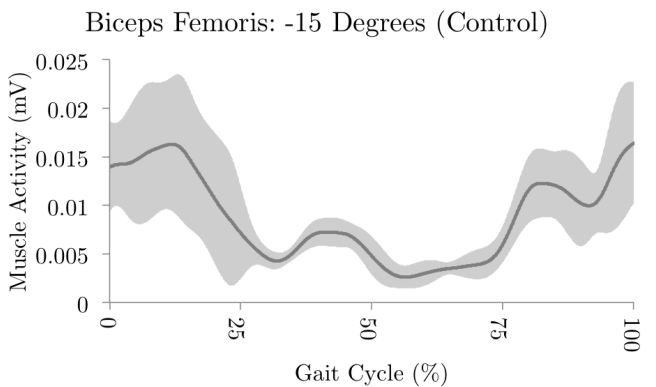


Figure A-27: Biceps femoris -15 degrees control

A.3 Ground Reaction Force

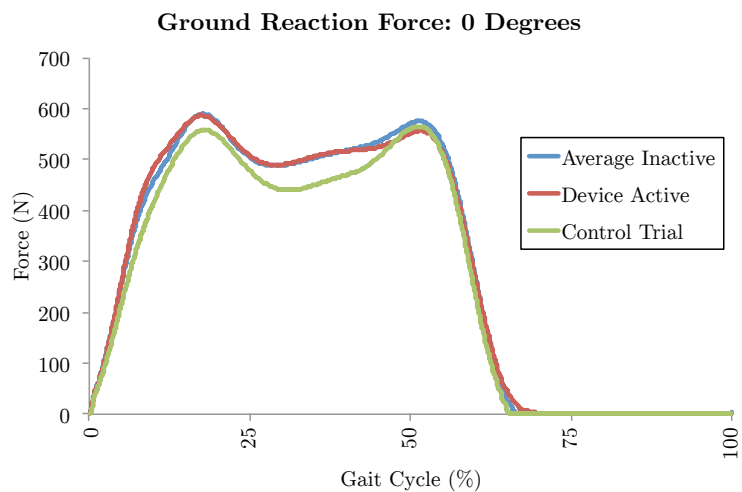


Figure A-28: Ground reaction force: 0 Degrees

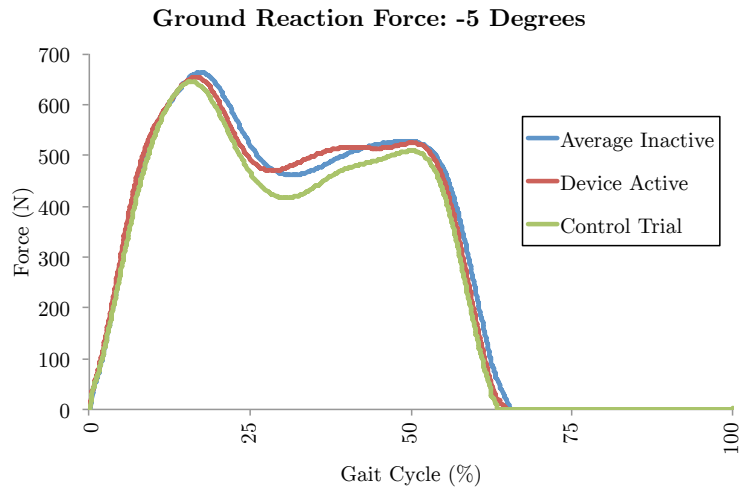


Figure A-29: Ground reaction force: -5 degrees

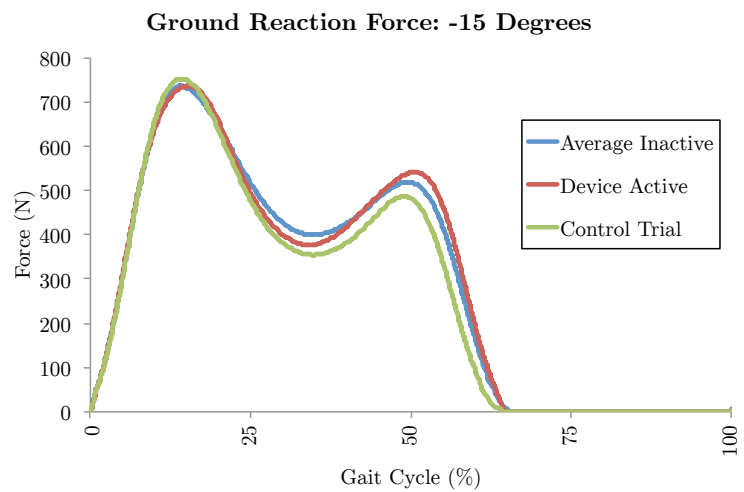


Figure A-30: Ground reaction force: -15 degrees

A.4 Joint Angles

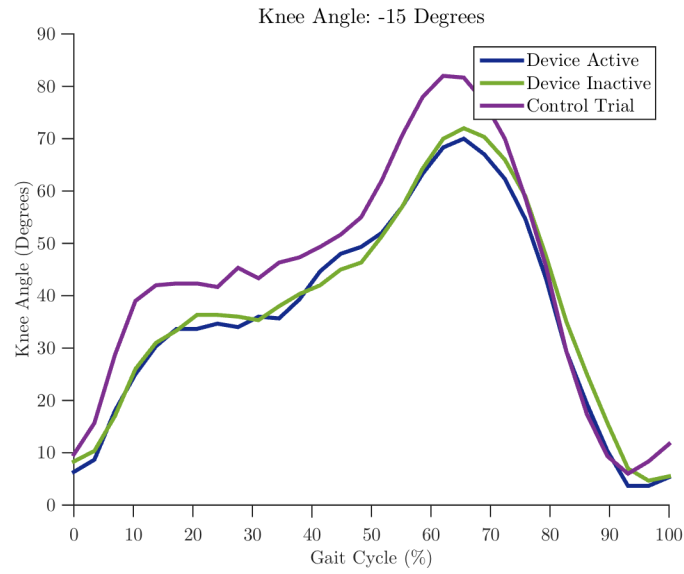


Figure A-31: Joint angle: -15 degrees

Appendix B

Bill of Materials

Part	Vendor	Part #	Cost (\$)	#	Total (\$)
Stock Piston and Cylinder Sets- 1.750" bore	Airpot	2KS444-CP	130	2	130
Low-Strength Steel Threaded Stud 10-32 Thread, 7" Long, Fully Threaded	McMaster	91565A868	5.75	1	5.75
Rod Alignment Coupler Brass, 5 Degree, 10-32 Thread, 0.63" Diameter, 1.79" Long	McMaster	7334K3	19.6	2	39.2
Pressure-Sealing Washer for Nuts and Washers Zinc-Plated Steel, Number 10 Screw Size, 0.194" ID, 0.469" OD	McMaster	93781A011	19.36	1	19.36
Grade 2 Steel Nylon-Insert Thin Hex Locknut Zinc-Plated, 10-32 Thread Size, 3/8" Wide, 11/64" High	McMaster	90633A411	3.18	1	3.18
Type 316 Stainless Steel Threaded Rod 2-56 Thread, 1 Foot Long	McMaster	93250A001	2.3	14	32.2
High-Strength 2024 Aluminum Rods	McMaster	86985K52	23.79	1	23.79
Parker Solenoid Cyclone Valve	Parker	75304 0122 B	150	1	150
Futuro Sport Hinged Knee Brace, Adjustable	Amazon	NA	21.29	2	42.58
Black Delrin Acetal Resin Tube 2-1/4" OD x 2" ID	McMaster	1830T289	14.59	2	29.18
Type 304 Smooth-Bore Seamless Stainless Steel Tubing 2-1/8" OD, 1.995" ID, .065" Wall	McMaster	89895K622	44.46	1	44.46
Medium-Pressure Brass Check Valve 1/4 NPT Female x 1/4 NPT Male, Buna-N Seal	McMaster	7768K22	10.22	1	10.22
DC 12V 250mA 3 Ways 2 Positions Solenoid Control Valve 3V1-06	Amazon	Amico s14050200am0105	11.41	1	11.41
Lowepro S&F Deluxe Technical Belt (S/M)	B&H Photo	LOSFDTBSM	35.13	1	35.13
Hardened Precision Steel Shaft 1/4" Diameter, 16" Length	McMaster	6061K416	7.69	2	15.38
Arduino Uno - R3	Sparkfun	DEV-11021	24.95	1	24.95
Blue 5-25V to 0.5-25V DC Boost-buck Converter 2A Step Up Down Voltage Regulator	Pro DC to DC	90637	9.89	2	19.78
Hyperion G3 Cx 2100 Mah 4S 14.8V 25C/45C Lithium Polymer Battery	Amazon	NA	37.95	1	37.95
Hyperion EOS 0606i AC/DC Digital Charger	Helipal	EOS0606iAD	99.9	1	99.99
High Strength 1144 Medium Carbon Steel Rod Extra-Strength, 1/4" Diameter	McMaster	6628K23	3.77	2	7.54
Hook and Loop Cable Tie with Buckle Nylon, 1" Wide, .095" Thick, 12" Overall Length (Black)	McMaster	3955T347	1.44	2	2.88
Push-to-Connect Tube Fitting for Air & Water Straight Adapter for 1/2" Tube OD x 1/4 NPT Male - Brass	McMaster	7880T134	3.62	2	7.24
Push-to-Connect Tube Fitting for Air & Water Straight Adapter for 1/4" Tube OD x 1/4 NPT Male - Brass	McMaster	7880T125	2.24	2	4.48
Push-to-Connect Tube Fitting for Air & Water Straight Adapter for 1/4" Tube OD x 1/8 NPT Male - Brass	McMaster	7880T124	2.24	2	4.48
Footswitch Pair	B&L Engineering	FSW	299.00	1	299.00
Total Cost of Prototyping					\$1100.13

Table B.1: Total Cost of Prototyping

Part	Vendor	Part #	Cost	#	Total
Stock Piston and Cylinder Sets- 1.750" bore	Airpot	2KS444-CP	130	1	130
Low-Strength Steel Threaded Stud 10-32 Thread, 7" Long, Fully Threaded	McMaster	91565A868	5.75	1	5.75
Rod Alignment Coupler Brass, 5 Degree, 10-32 Thread, 0.63" Diameter, 1.79" Long	McMaster	7334K3	19.6	2	39.2
Pressure-Sealing Washer for Nuts and Washers Zinc-Plated Steel, Number 10 Screw Size, 0.194" ID, 0.469" OD	McMaster	93781A011	19.36	1	19.36
Grade 2 Steel Nylon-Insert Thin Hex Locknut Zinc-Plated, 10-32 Thread Size, 3/8" Wide, 11/64" High	McMaster	90633A411	3.18	1	3.18
Type 316 Stainless Steel Threaded Rod 2-56 Thread, 1 Foot Long	McMaster	93250A001	2.3	5	11.5
Parker Solenoid Cyclone Valve	Parker	75304 0122 B	150	1	150
Lowepro S&F Deluxe Technical Belt (S/M)	B&H Photo	LOSFDTBSM	35.13	1	35.13
Futuro Sport Hinged Knee Brace, Adjustable	Amazon	NA	21.29	2	42.58
Black Delrin Acetal Resin Tube 2-1/4" OD x 2" ID	McMaster	1830T289	14.59	2	29.18
Arduino Uno - R3	Sparkfun	DEV-11021	24.95	1	24.95
Blue 5-25V to 0.5-25V DC Boost-buck Converter 2A Step Up Down Voltage Regulator	Pro DC to DC	90637	9.89	2	19.78
Hyperion G3 Cx 2100 Mah 4S 14.8V 25C/45C Lithium Polymer Battery	Amazon	NA	37.95	1	37.95
High Strength 1144 Medium Carbon Steel Rod Extra-Strength, 1/4" Diameter	McMaster	6628K23	3.77	2	7.54
Hook and Loop Cable Tie with Buckle Nylon, 1" Wide, .095" Thick, 12" Overall Length (Black)	McMaster	3955T347	1.44	2	2.88
Push-to-Connect Tube Fitting for Air & Water Straight Adapter for 1/2" Tube OD x 1/4 NPT Male - Brass	McMaster	7880T134	3.62	2	7.24
Push-to-Connect Tube Fitting for Air & Water Straight Adapter for 1/4" Tube OD x 1/8 NPT Male - Brass	McMaster	7880T124	2.24	2	4.48
High Flow Check Valve with Barbed End	Qosina	91030	1	2	2
Footswitch Pair	B&L Engineering	FSW	299	1	299
Cost of Final Prototype					\$871.7

Table B.2: Cost of Final Prototype

Appendix C

Engineering Drawings

This appendix includes engineering drawings for the major components of the air spring. All dimensions listed are in mm.

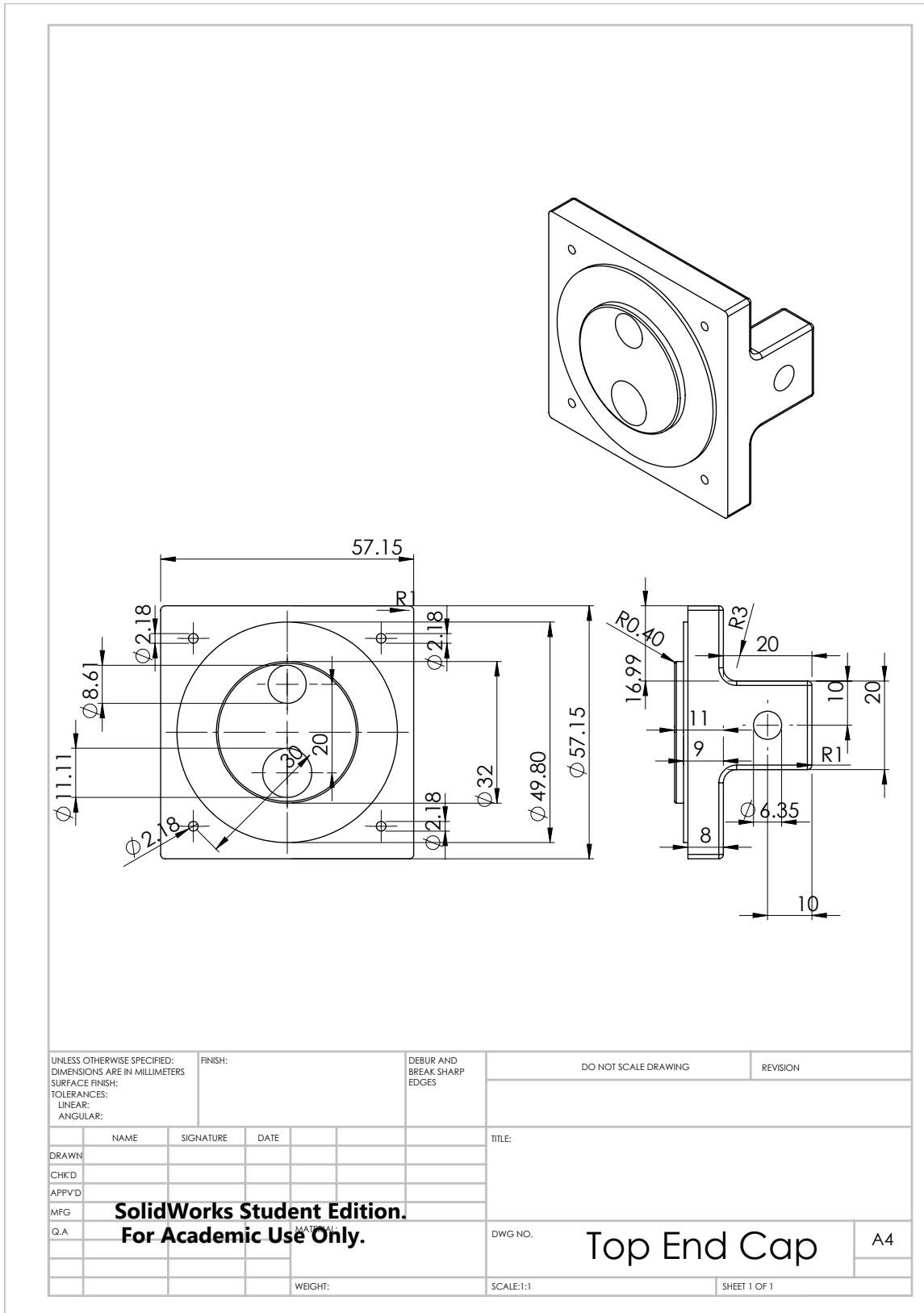


Figure C-1: Engineering drawing: top air spring end cap

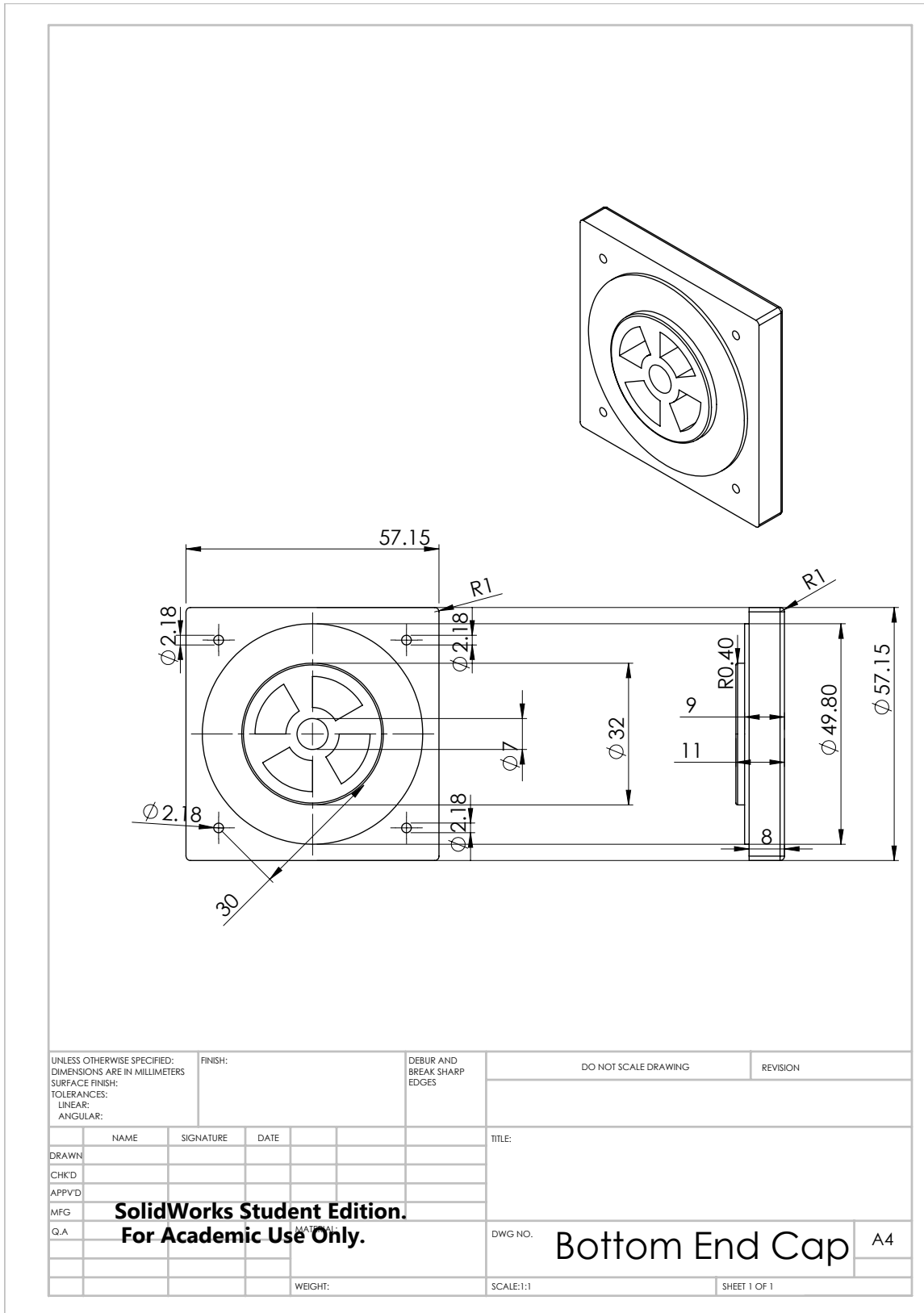


Figure C-2: Engineering drawing: bottom air spring end cap

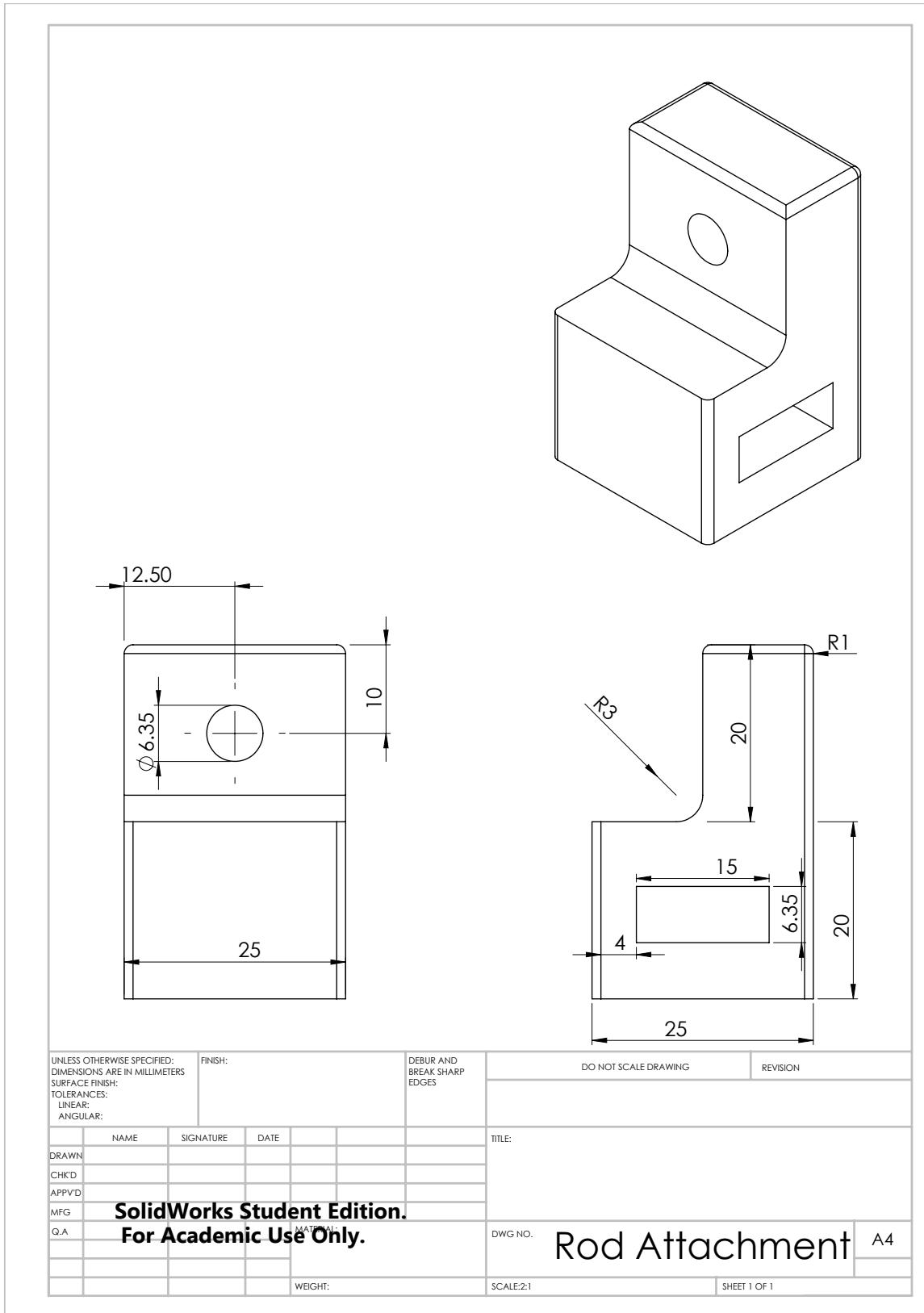


Figure C-3: Engineering drawing: rod attachment piece

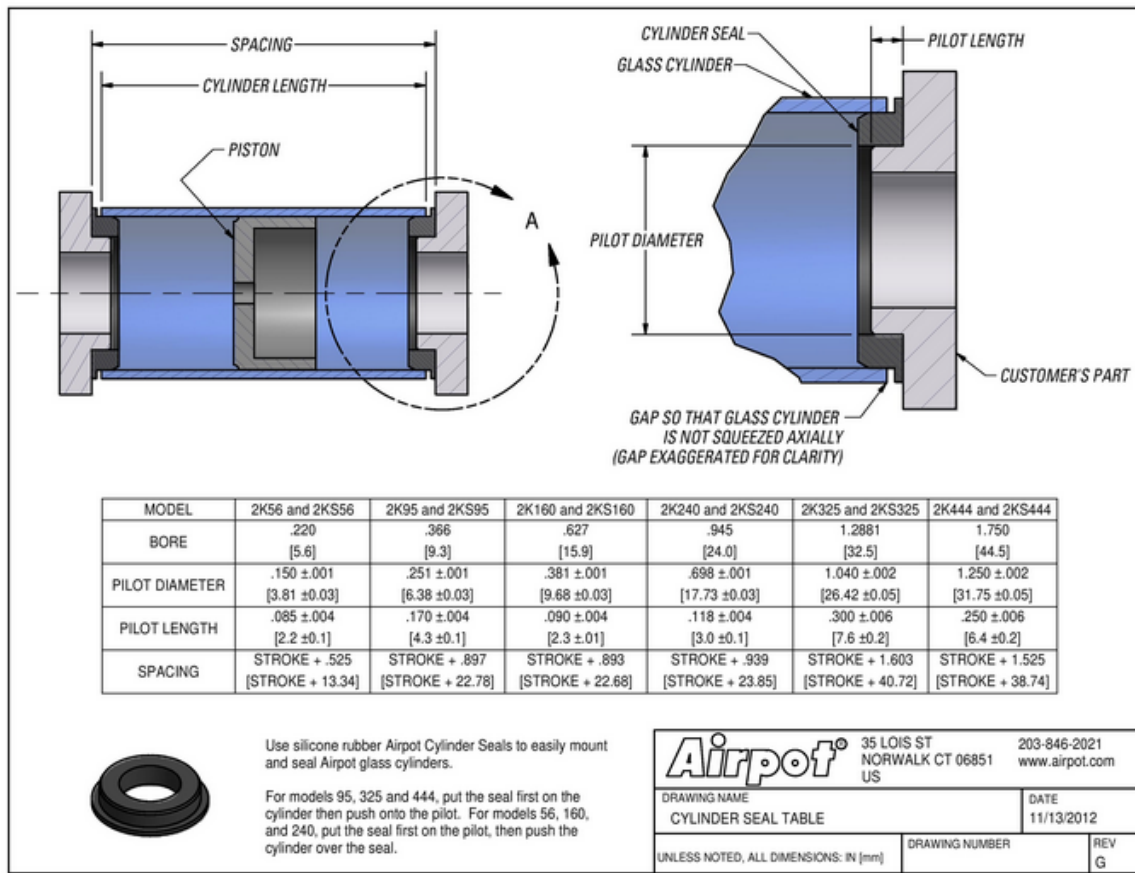


Figure C-4: Cylinder piston datasheet showing part dimensions [16]

Appendix D

Code

```
// Arduino Control of Solenoid Valve
// Emily Rogers

int mosfetPin = 3; // Mosfet pin for solenoid control
int BNCsignal = 2; // Sending signal to BNC cable during testing
int foot0 = 0; // Right footswitch on pin 0
int foot1 = 1; // Left footswitch on pin 1
int foot0_sensor; // Right footswitch sensor value
int foot1_sensor; // Left footswitch sensor value
int valvestate = 0; // Valvestate to keep track of which foot is active
int counter = 0; // Set counter to 0 initially

void setup() {
    pinMode(mosfetPin, OUTPUT); // Set mosfetPin as output
    pinMode(foot0, INPUT); // Set foot switches as inputs
    pinMode(foot1, INPUT); // Set foot switches as inputs
    pinMode(BNCsignal, OUTPUT); // Set BNCsignal as output
}

void loop() {
    while(counter > 100) { // If both feet have been on ground for more
        than 1 second
        foot1_sensor = analogRead(foot1); // Read value from foot switch
```

```

foot0_sensor = analogRead(foot0); // Read value from foot switch
if(foot1_sensor < 1000) { // If foot1 lifted off ground
    digitalWrite(mosfetPin, LOW); // If foot1 lifted off ground, open
    valve
    digitalWrite(BNCsignal, LOW); // Send same signal to BNC cable
    for data collection
    valvestate = 0; // Set valvestate to 0
    counter = 0; // Set counter to 0
}
if(foot0_sensor < 1000) { // If foot0 lifted off ground
    digitalWrite(mosfetPin, HIGH); // If foot0 lifted off ground,
    open valve
    digitalWrite(BNCsignal, HIGH); // Send same signal to BNC
    cable for data collection
    valvestate = 1; // Set valve state to 1
    counter = 0; // Set counter to 0
}
}

foot1_sensor = analogRead(foot1); // Read value from foot switch
foot0_sensor = analogRead(foot0); // Read value from foot switch

if (valvestate == 0) { // If foot0 was recently detected
    if (foot1_sensor > 1000) { // If heel strike is detected on
        foot1
        digitalWrite(mosfetPin, HIGH); // If foot1 heelstrike detected
        , close valve
        digitalWrite(BNCsignal, HIGH); // Send same signal to BNC
        cable for data collection
        valvestate = 1; // Set valve state to 1
    }
}
else { // If foot1 was recently detected
    if (foot0_sensor > 1000) { // If heel strike is detected on foot0
        digitalWrite(mosfetPin, LOW); // If foot0 heelstrike detected,
        open valve
}

```

```
digitalWrite(BNCsignal, LOW); // Send same signal to BNC cable
for data collection
valvestate = 0; // Set valve state to 0
}
}

if (foot1_sensor > 1000 && foot0_sensor > 1000) {
    counter++; // While both feet on ground, increase counter
}
delay(10);
}
```


Appendix E

Survey Data

This section lists the survey questions and responses from the user needs research. The survey was administered online and participation was voluntary.

1. What age category do you fall into?

- <20 years old
- 20-30 years old
- 30-45 years old
- 45-60 years old
- 60+ years old

2. Describe your physical activity level

- Low (<2 hours/week)
- Moderate (2-5 hours/week)
- High (5-10 hours/week)
- Very High (>10 hours/week)

3. Do you currently use any assistive device while hiking/walking?

- Yes

- No

4. If yes, what do you use?

- Hiking poles
- Knee brace
- Other

5. Do you experience knee pain during or after hiking?

- During
- After
- Both

6. Have you ever injured your knee while hiking?

- Yes
- No

7. In your opinion, would it be worthwhile to carry slightly more weight uphill (2 kg) in order to reduce strain on knees while walking downhill?

- Yes, if it a long and steep descent
- Yes, almost always
- No

8. The information I provided may be used anonymously for research purposes, as well as presented in written academic documents and presentations

- Agree
- Disagree

Activity Level

Very High	20
High	48
Moderate	21
Low	3

Age

<20	11
20-30	36
30-45	10
35-60	31
60+	6

Do you currently use an assistive device while hiking?

No	52
Yes	42

Do you experience knee pain while hiking?

During	31
After	14
Both	30
No	19

Have you injured your knee while hiking?

No	78
Yes	15

Would you use an assistive exoskeleton?

No	19
Yes, almost always	12
Yes, if long and steep descent	63

References

- [1] “Trekking poles [image],” Online, url: <http://activeadventures.com/new-zealand/about/activities/hiking/multiday-tramp-gearlist>.
- [2] *FUTURO Hinged Knee Brace*, 3M.
- [3] G. Howatson, P. Hough, J. Pattison, J. A. Hill, R. Blagrove, M. Glaister, K. G. Thompson, and others, “Trekking poles reduce exercise-induced muscle injury during mountain walking,” *Med Sci Sports Exerc*, vol. 43, no. 1, pp. 140–5, 2011.
- [4] S. Najibi and J. P. Albright, “The use of knee braces, part 1: Prophylactic knee braces in contact sports,” *The American Journal of Sports Medicine*, vol. 33, no. 4, pp. 602–611, Apr. 2005.
- [5] McLaren, “Bionex: the next step in mechanical motion,” pp. 1–21, 2012.
- [6] Q. Li, V. Naing, and J. M. Donelan, “Development of a biomechanical energy harvester,” *Journal of NeuroEngineering and Rehabilitation*, vol. 6, no. 1, pp. 1–12, Jun. 2009. [Online]. Available: <http://link.springer.com/article/10.1186/1743-0003-6-22>
- [7] M. Yarri, “An exoskeleton device to assist in downhill walking,” *Harvard University School of Engineering and Applied Sciences*, 2014.
- [8] C. for Disease Control and Prevention, “Osteoarthritis,” Online, url: <http://www.cdc.gov/arthritis/basics/osteoarthritis.htm>.
- [9] *Video Analysis Software*, Kinovea.
- [10] A. N. Lay, C. J. Hass, and R. J. Gregor, “The effects of sloped surfaces on locomotion: A kinematic and kinetic analysis,” *Journal of Biomechanics*, vol. 39, no. 9, pp. 1621–1628, Jan. 2006. [Online]. Available: <http://www.jbiomech.com/article/S0021929005002150/abstract>
- [11] A. N. Lay, C. J. Hass, T. Richard Nichols, and R. J. Gregor, “The effects of sloped surfaces on locomotion: An electromyographic analysis,” *Journal of Biomechanics*, vol. 40, no. 6, pp. 1276–1285, 2007. [Online]. Available: <http://www.sciencedirect.com/science/article/pii/S0021929006001977>

- [12] R. C. Browning, J. R. Modica, R. Kram, and A. Goswami, “The effects of adding mass to the legs on the energetics and biomechanics of walking,” *Medicine and Science in Sports and Exercise*, vol. 39, no. 3, pp. 515–525, Mar. 2007.
- [13] A. M. Grabowski and H. M. Herr, “Leg exoskeleton reduces the metabolic cost of human hopping,” *Journal of Applied Physiology (Bethesda, Md.: 1985)*, vol. 107, no. 3, pp. 670–678, Sep. 2009.
- [14] A. L. Desbiens, M. T. Pope, D. L. Christensen, E. W. Hawkes, and M. R. Cutkosky, “Design principles for efficient, repeated jumpgliding,” *Bioinspiration & Biomimetics*, vol. 9, no. 2, p. 025009, Jun. 2014. [Online]. Available: <http://iopscience.iop.org/1748-3190/9/2/025009>
- [15] S. Pugh, “Concept selection: a method that works,” *Proceedings of the International Conference on Engineering Design*, vol. 107, no. 3, pp. 497–506, 1981.
- [16] *Stock Piston and Cylinder Sets*, Airpot Corporation, 11 2012, rev. G.
- [17] *High Flow Check Valve with Barbed End*, Qosina.
- [18] *Lowepro S and F Deluxe Technical Belt (S/M)*, B and H Photo.
- [19] *Footswitch Pair*, B and L Engineering.
- [20] *Parker Solenoid Cyclone Valve*, Parker.
- [21] “Anatomical leg diagram [image],” Online, url: <https://s-media-cache-ak0.pinimg.com/originals/24/d1/aa/24d1aa8ebeaa22d2df62522ee9139411.jpg>.